In presenting the dissertation as a partial fulfillment of the requirements for an advanced degree from the Georgia Institute of Technology, I agree that the Library of the Institution shall make it available for inspection and circulation in accordance with its regulations governing materials of this type. I agree that permission to copy from, or to publish from, this dissertation may be granted by the professor under whose direction it was written, or, in his absence, by the dean of the Graduate Division when such copying or publication is solely for scholarly purposes and does not involve potential financial gain. It is understood that any copying from, or publication of, this dissertation which involves potential financial gain will not be allowed without written permission.

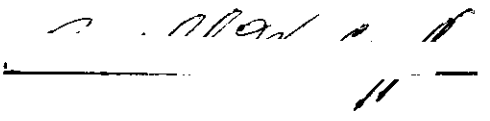

CROSS-CHANNEL TRANSFER OF LINEAR MOMENTUM

A THESIS

Presented to

The Faculty of the Graduate Division

by

Russell William Cruff

In Partial Fulfillment

of the Requirements for the Degree

Master of Science in the School of Civil Engineering

Georgia Institute of Technology

December, 1963

CROSS-CHANNEL TRANSFER OF

LINEAR MOMENTUM

Approved:

Date Approved by Chairman: Nov. 14, 1963

ACKNOWLEDGMENTS

The writer is grateful to all those who made this thesis possible, and expresses sincere appreciation to Dr. M. R. Carstens, thesis advisor, for his guidance and assistance throughout this study. Further appreciation is expressed to Mr. H. J. Tracy, Hydraulic Engineer with the U. S. Geological Survey, for his thoughtful review of the work.

Dr. Carstens, Dr. Paul G. Mayer, and Professor C. S. Martin served as members of the thesis reading committee.

The writer wishes also to thank the U. S. Geological Survey for its assistance and material support, which has made his studies and this thesis at the Georgia Institute of Technology possible.

Permission to use the previously collected data, used in this study, was granted by the U. S. Geological Survey.

TABLE OF CONTENTS

LIST OF TABLES

LIST OF FIGURES

LIST OF FIGURES (Continued)

LIST OF SYMBOLS

a constant

A area of cross-section

B total width of channel bottom

F_a apparent shear force

F'_a apparent shear force for incremental distance in the longitudinal direction

P wetted perimeter

R hydraulic radius, A/P

$\mathbb{R}$ Reynolds number

S_o slope of the uniform flow

u velocity at a point

u_* local shear velocity, $\sqrt{\tau_o/\rho}$

$\bar{u}_*$ average shear velocity, $\sqrt{\bar{\tau}_o/\rho}$

U average velocity in the cross-section

y distance above the channel bottom

y_o uniform flow depth

z distance from the wall in the lateral direction

β correction for the variation in shear stress along the solid boundary

γ specific weight of fluid

$\bar{\epsilon}$ correction for the apparent shear at the free surface of an open channel

θ slope angle

κ Von Kármán's constant

ν kinematic viscosity

LIST OF SYMBOLS (Continued)

ρ fluid mass density

τ_o local boundary shear stress

$\bar{\tau}_a$ average apparent shear stress

$\bar{\tau}_o$ average boundary shear stress

τ'_o two-dimensional shear stress, $\gamma\, y_o S_o$

SUBSCRIPTS, UNLESS DEFINED ABOVE

x longitudinal direction

y vertical direction

z lateral direction

1 upstream section

2 downstream section

SUPERSCRIPTS, UNLESS DEFINED ABOVE

– time average

SUMMARY

All shear flows are characterized by a net transfer of forward linear momentum from regions of higher linear momentum to regions of lower linear momentum.

In open channels there is also a lateral cross-channel transfer of linear momentum. This lateral transfer can be transfer from a main channel section to an overbank section or it can be transfer from the central region to the vertical wall regions in a rectangular channel.

The object of this investigation was to study this lateral transfer of momentum from the central region to the vertical wall regions in smooth rectangular channels. This was done by means of first determining the shear stress along the channel periphery and then using this shear stress to solve for the lateral cross-channel transfer of linear momentum using the momentum equation.

The data used for this investigation was obtained previously and partially reported by Tracy and Lester in U. S. Geological Survey Water-Supply Paper 1592A. Twenty six tests were used with test conditions covering a range of depth-to-width ratios from 0.026 to 0.211, Reynolds numbers from 43,770 to 726,900, average channel velocity from 0.77 to 7.70 feet per second and two-dimensional shear stress from 0.0038 to 0.2325 pounds per square foot.

The shear stress along the channel periphery was computed by two methods. One method being that using the Preston-tube technique and the other using Von Kármán's logarithmic velocity law. From these

computed shear stresses the shear stress distributions, the maximum shear stress, and the average shear stresses for the channel bottom and walls were found and plotted. The depth-to-width ratio of the channel cross-section was found to be the only flow characteristic which affected the boundary shear stress (distribution, maximum, and average) for smooth boundaries and a modest range of Reynolds numbers. A central region with two-dimensional shear stress was found by the writer for smooth rectangular channels with depth-to-width ratios less than 0.08. In other words, the region in which the shear stress is affected by the wall extends a distance of about six times the flow depth laterally from the wall.

CHAPTER I

INTRODUCTION

Linear Momentum Transfer

All shear flows are characterized by a net transfer of forward linear momentum from regions of higher linear momentum to regions of lower linear momentum.

The simplest example is that of laminar flow in a pipe. In this case linear momentum is transported toward the wall region by a molecular transfer mechanism. With turbulent flow in a pipe the linear momentum is transferred to the wall region by the action of turbulence.

Another example is that of overbank flow in which linear momentum is transported from the main channel section to the overbank section both by turbulence and by vertically oriented giant eddies (at least with shallow depths in the overbank section), which form at the junction plane of the main channel and overbank sections. The existence of these vertically oriented giant eddies was observed by Wilroy (1) and Rodriguez-Diaz (2) in their experiments with the hydraulic jump in a nonrectangular open channel. The channel used by Wilroy and Rodriguez-Diaz had vertical walls with a cross-channel slope in the bottom resulting in a variable depth across the channel. For a hydraulic jump to occur in such a channel a massive transfer of linear momentum from the deeper to the shallower portion is required. Rodriguez-Diaz observed that under certain conditions turbulence plus well-behaved cross currents were sufficient

to effect the required transfer. On the other hand if the required rate of transfer were too great, vertically oriented giant eddies formed which were capable of massive transport of linear momentum toward the shallower side.

Another mechanism which can transport linear momentum consists of line vortices alined with axes along the channel. The superposition of these line vortices on the flow is called secondary circulation. Prandtl (3) presented a hypothesis about the location of these vortex pairs in various noncircular conduits. This secondary circulation is an effective supplement to turbulence in transferring linear momentum toward the wall regions in flow in polygonal conduits.

In a rectangular open channel, linear momentum must be transferred both downward toward the floor and laterally toward the walls. The lateral transport is necessitated by the existence of boundary shear on the wall. With two-dimensional flow, the net transport would be only in one direction, that is, toward the floor. Conceptually the flow is divided into two three-dimensional flow regions in the vicinity of the walls and into a two-dimensional flow region in the central portion of the channel. The flow characteristics, including turbulence in the two-dimensional region, have been experimentally investigated by Laufer (5) for flow in a rectangular smooth conduit. The existence of a three-dimensional flow region near the wall is known to be reflected in the following flow characteristics -- mean velocity, turbulence, apparent shear stresses, and boundary shear stress.

From the engineering standpoint the flow characteristic of prime interest is that of boundary-shear stress. For example, most engineering

analyses is gross-streamtube analysis, for which the total boundary-shear force is required. As a further example, movement of particles on the bed and on the banks of a stream is directly related to the boundary-shear stress. Determination of the boundary-shear stress distribution and the cross-channel transfer of linear momentum in rectangular open channels is the object of this investigation.

Linear Momentum Equation

The linear momentum equation for steady flow is simply:

$$\begin{bmatrix}\text{Summation of the}\\ \text{external forces}\\ \text{on a free body}\end{bmatrix} = \begin{bmatrix}\text{Rate of transport}\\ \text{of linear momentum}\\ \text{out of the free body}\end{bmatrix} - \begin{bmatrix}\text{Rate of transport}\\ \text{of linear momentum}\\ \text{into the free body}\end{bmatrix} \quad (1)$$

For purpose of analysis a rectangular parallelepiped as shown in Figure 1 is chosen as a fluid free body. Face 1 is at the junction of the fluid and the bed. Face 2 is the free surface. Face 3 is a vertical plane along the centerline. Face 4 is a vertical plane parallel to the centerline at a distance of $(\frac{1}{2}B) - z$ from the centerline. Faces 5 and 6 are the end faces of the free body and are separated by the axial distance dx. The linear momentum equation in the x-direction, along the axis of the channel, is formulated for steady uniform flow.

The external forces in the x-direction on the free body are as follows: (a) the pressure forces on faces 5 and 6; (b) the boundary-shear force on face 1, $dx \int_{\frac{1}{2}B}^{z} \tau_{ob}(-\,dz)$; and (c) the weight force, $\gamma[(\frac{1}{2}B) - z](y_o \sin\theta)dx$. Since the flow is uniform the pressure force on face 5 exactly equals that on face 6.

The linear momentum transport terms are as follows: (a) The linear momentum transport rate out through face 6 exactly equals the

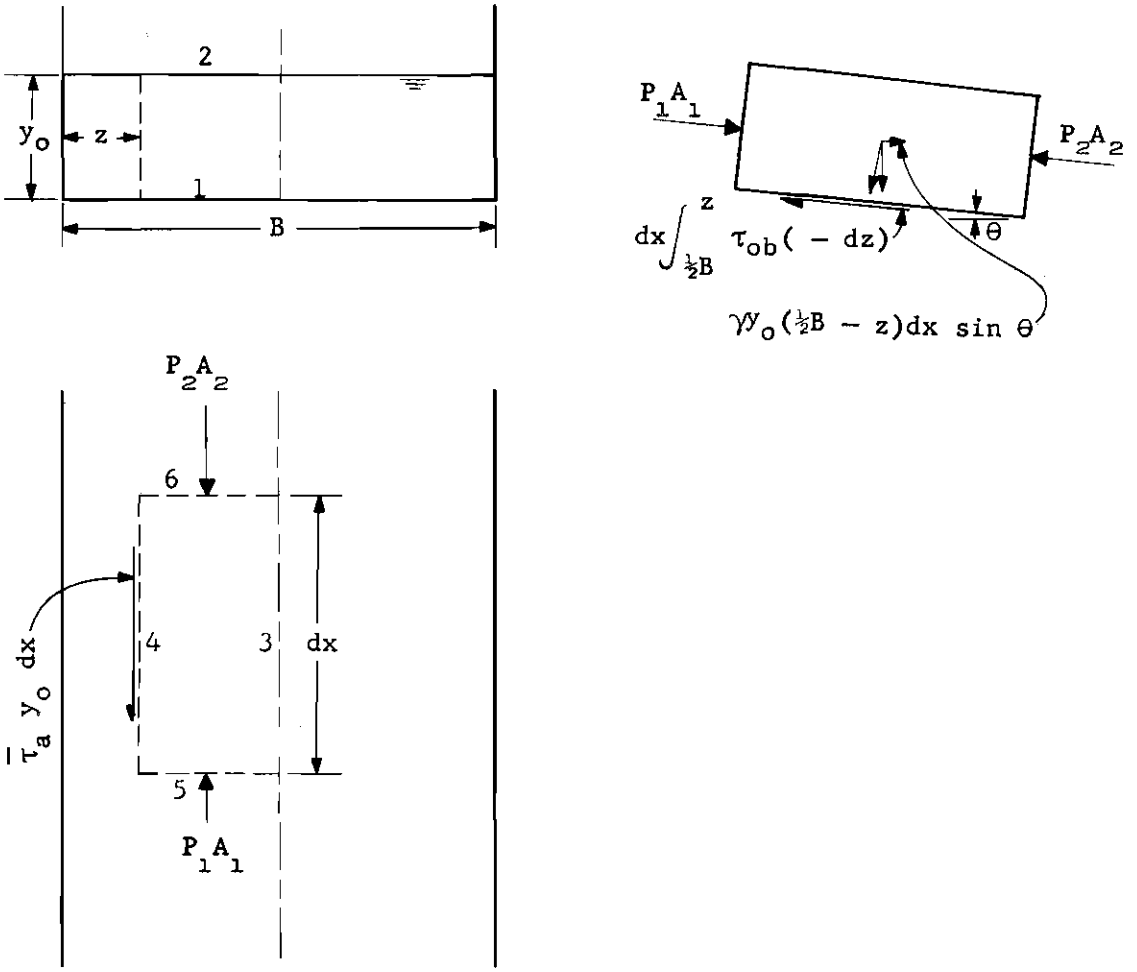

Figure 1. Definition Sketch of Forces in the Momentum Equation.

transport rate in through face 5. (b) The net transport rate of linear momentum through face 3 by turbulent eddies is zero by virture of the location of face 3 on the axis of symmetry. (c) The linear momentum transport rate out through face 4 is affected both by turbulent eddies and secondary circulation. The traditional treatment of the linear momentum transport term through face 4 is to transfer this term to the left side of Equation (1). Upon performing this operation, the term can be

considered as being apparent shear force, $\bar{\tau}_a\ y_o\ dx$.

The linear momentum equation is:

$$- dx\int_{\frac{1}{2}B}^{z} \tau_{ob}(-dz) - \bar{\tau}_a\ y_o\ dx + \gamma[(\tfrac{1}{2}B) - z](y_o \sin\theta)dx = 0 \qquad (2)$$

In which B = total channel width

x = distance in the longitudinal direction

y_o = uniform flow depth

z = distance laterally from the wall

γ = fluid specific weight

θ = slope angle

ρ = fluid mass density

τ_{ob} = shear stress on the channel bottom and

$\bar{\tau}_a$ = average apparent shear stress.

For the entire channel, that is z = 0, Equation (2) reduces to:

$$- \bar{\tau}_{ob}(\tfrac{1}{2}B)dx - \bar{\tau}_{ow}\ y_o\ dx + \gamma(\tfrac{1}{2}B)\ y_o \sin\theta\ dx = 0$$

in which $\bar{\tau}_{ob}$ is the mean shear stress on the bed and $\bar{\tau}_{ow}$ is the mean shear stress on the wall. Simplifying Equation (2)

$$- \bar{\tau}_{ob}\ (B) - \bar{\tau}_{ow}(2y_o) + \gamma(By_o)\ S_o = 0 \qquad (3)$$

in which S_o is the bottom slope, sin θ. The common procedure is to obtain the mean value over the entire boundary rather than averaging the bottom and walls separately. In which case Equation (2) can be simplified as follows:

$$-\bar{\tau}_o\ (B + 2y_o) + \gamma(B\ y_o)S_o = 0$$

or

$$\bar{\tau}_o = \gamma(A/P)S_o = \gamma R\ S_o \qquad (3a)$$

in which $\bar{\tau}_o$ is the mean shear stress averaged over the entire boundary, A is the cross-sectional area, By_o, P is the wetted perimeter, $B + 2y_o$, and R is the hydraulic radius, A/P.

Method and Scope of the Investigation

The main objective of this investigation was to analyze the data previously obtained by the United States Geological Survey in the Georgia Institute of Technology Hydraulics Laboratory. Particular attention is given to the cross-channel transfer of linear momentum. These data have been partially reported by Tracy and Lester (5). The major part of the writer's analysis was based on the study of the shear stress distribution along the channel bottom and walls from which the cross-channel transfer of linear momentum can be computed using Equation (2).

Review of the Literature

The writer knows of no literature which pertains totally to this cross-channel transfer of linear momentum and there have been very few publications which totally pertain to shear stress distribution. Most investigations into the determination of the shear stress in open channels have either been directed toward methods of measuring shear stress or else they have been done as a side product of a larger investigation. The major portion of these investigations have been done in conjunction

with a study of sediment transport. This is partly due to the fact that a knowledge of the shear stress, or tractive force as it is usually referred to in sedimentation studies, is required for investigation of channel stability.

Keulegan (6), in 1938, using Von Kármán's velocity law,

$$\frac{u}{u_*} = a + \frac{1}{\kappa} \ell n \left(\frac{y u_*}{\nu}\right) \tag{4}$$

derived the expression for the mean velocity in a trapezoidal cross-section

$$\frac{U}{\bar{u}_*} = a - \frac{1}{\kappa} + \frac{1}{\kappa} \ell n \left(\frac{R \bar{u}_*}{\nu}\right) + \frac{1}{\kappa} \beta - \bar{\epsilon} \frac{U}{\bar{u}_*} \tag{5}$$

in which a = constant

R = hydraulic radius

u = velocity at a point

U = average velocity for the cross-section

u_* = shear velocity, $\sqrt{\tau_o/\rho}$

$\bar{u}_*$ = average shear velocity, $\sqrt{\bar{\tau}_o/\rho}$

y = distance above the channel bottom

β = correction for the variation in shear along the solid boundary

$\bar{\epsilon}$ = correction for apparent shear at the free surface

κ = Von Kármán's constant and

ν = kinematic viscosity.

Keulegan states that the correction for apparent shear at the free surface may be neglected and that the correction for the variation in shear along the solid boundary of rectangular channels can be taken as 0.1. He shows

that the hydraulic radius can be used in Equation (5) as the characteristic length for the cross-section. Using Bazin's data, Keulegan also computed the shear velocity for points along the bottom and the walls of the channel by means of Equation (5).

Lane (7) made an unsuccessful attempt to determine the shear distribution by a mathematical process using Von Kármán's logarithmic distribution and boundary layer theory. Mathematical solutions of a supposedly analogous differential equation were obtained for a rectangular channel with a depth-to-width of 1 to 2. His results show a maximum shear stress on the bottom approaching $\gamma\ y_o\ S_o$ (the two-dimensional shear stress) and a maximum of $0.76\ \gamma\ y_o\ S_o$ on the walls.

Leutheusser (8) in a study of turbulent flow in rectangular ducts determined the shear stress around the periphery of rectangular ducts with aspect ratios of 1 to 3 and 1 to 1. He computed the shear stress using Preston's technique. His tests were made at Reynolds numbers ranging from 34,000 to 92,000. He found a variation in the shear stress distribution with Reynolds number.

Hsu (9) extended J. H. Preston's technique for the determination of local skin friction in pipes to that for boundary layer flow with adverse pressure gradients. He was able to check Preston's calibration curve almost identically for round-surface pitot tubes on flat surfaces with zero pressure gradient as well as with adverse pressure gradients.

Hwang and Laursen (10) show that the methods developed by Preston and Hsu give satisfactory results even in channels with rough boundaries.

CHAPTER II

LABORATORY EQUIPMENT

General

All tests for this investigation were made previously, by the research personnel of the United States Geological Survey, in the Hydraulics Laboratory, School of Civil Engineering, Georgia Institute of Technology, Atlanta, Georgia. As stated before the results were partially reported by Tracy and Lester (5).

The Flume

The laboratory tests were made in a steel flume 3.5 feet wide, 18 inches deep (see Figure 2(a)) and 80 feet long. The flume is supported at its midpoint on a fixed pivot and at the ends by pairs of screw jacks. An electric motor at the pivot drives the two pairs of jacks simultaneously through torque tubes of equal length. The drive mechanism also furnishes a method for the determination of the flume slope. The number of turns made by the torque tubes from the level flume position is indicated by a mechanical counting device. The vertical displacement of the two ends of the flume for various counter readings has been measured by precise levels. A calibration of counter reading against flume slope has been prepared from this data and the measurement of the distance between the two end points.

Two longitudinal, variable-depth, built up steel beams furnish the principal support for the flume box. Two four-inch channels placed

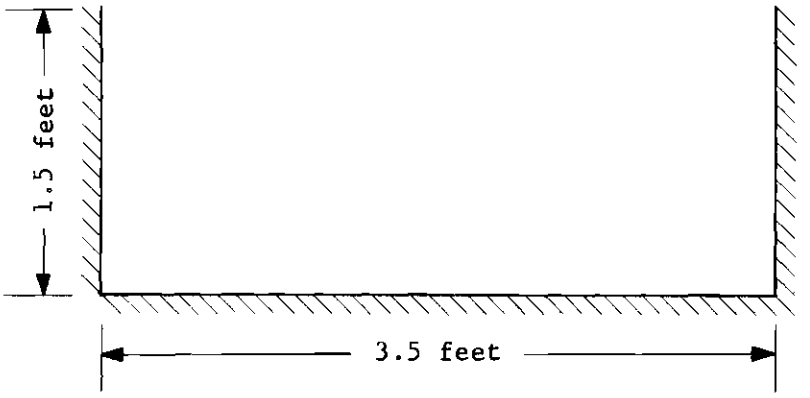

(a)

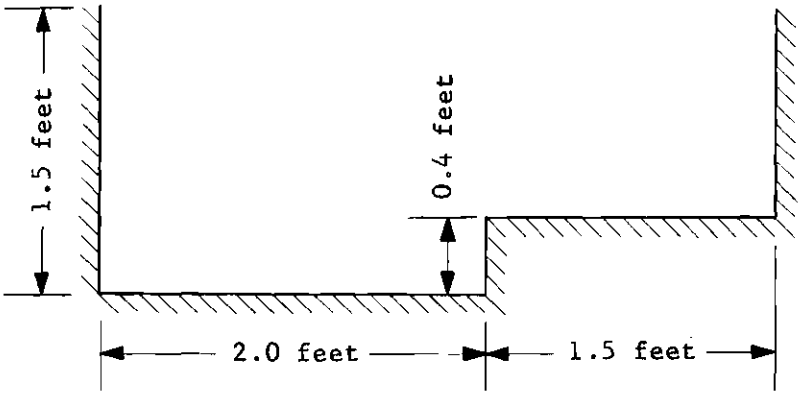

(b)

Figure 2. Channel Cross-Sections

back-to-back are welded in place on top and across the beams at three-foot intervals. Five lengths of threaded 3/4-inch rod, inserted

vertically between each channel pair and spread at equal intervals, are held in place by nuts bearing on the top and bottom of the channels. The rods project to a height of about three inches above the top of the channels, and form bearing supports for five small car channels which extend the length of the flume. The flume floor is bolted directly to the car channels. Small irregularities in the flume floor as well as the curvature due to the dead weight deflection of the supporting beams may be removed by adjustments in the height of the tops of the threaded rods. The side walls are supported by channel lengths welded to the angles that form the bottom support for the side plates. The channel lengths are vertical and on three foot centers. Bolts tapped through the channels permit slight adjustments to be made in the position of the side walls. The inner flume surfaces are covered by one seal coat and two coats of synthetic enamel, applied by brush.

Before tests were made in the flume, the bottom and sides of the flume were adjusted to make them as plane as possible. Precise levels were run to determine the variation of the bottom and where necessary, the bottom elevation adjusted by means of the supporting rods under the flume floor. Figure 3 shows the average configuration of the bottom and sides of the flume after the adjustments were made.

The deflection characteristics of the flume under various depths of flow are shown in Figure 4. The deflection is small enough to be unimportant except at the extreme downstream end of the flume at depths greater than one-half foot of water.

Water surface levels are read by point gages from a carriage which moves on rails mounted on the top of the sidewalls of the flume. Piezometer

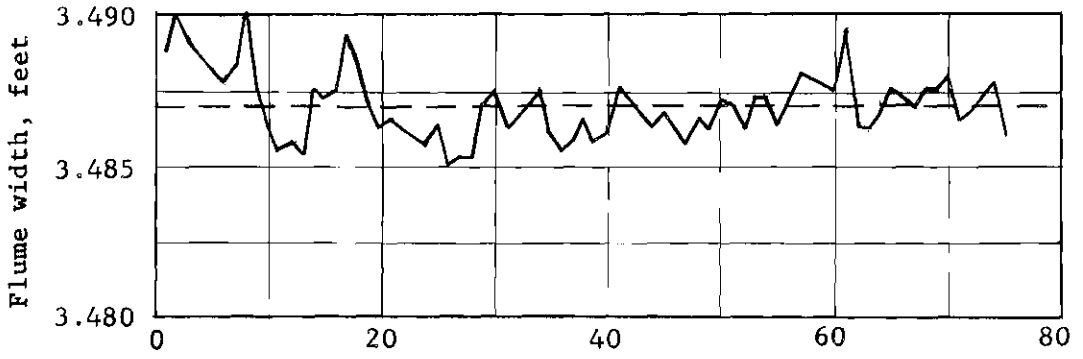

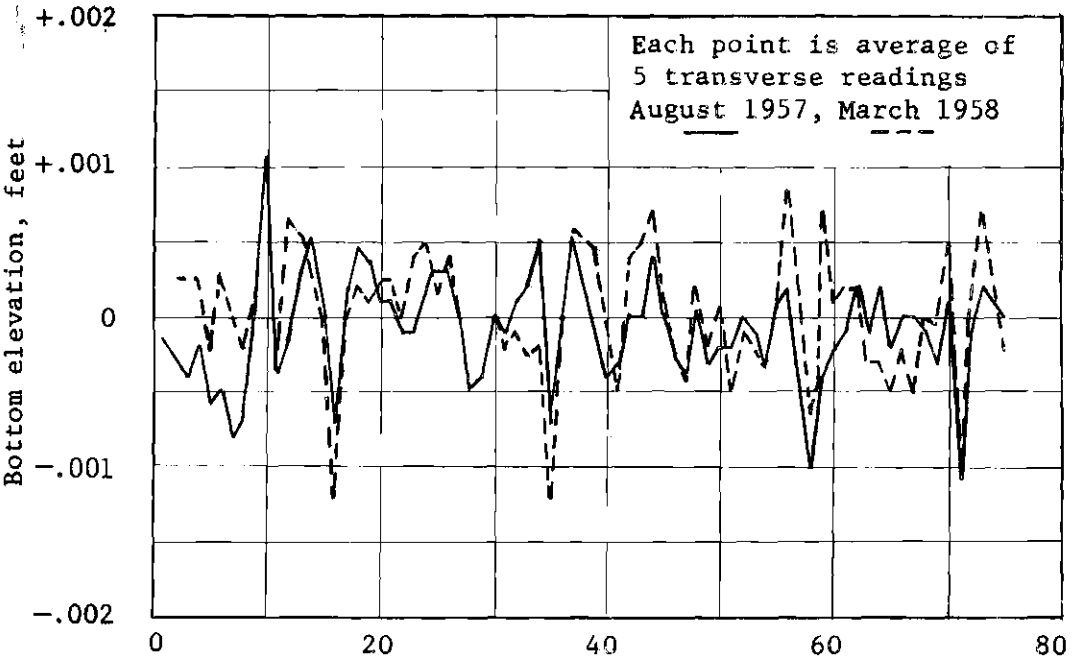

Figure 3. Average Configuration of Bottom and Sides of Flume.

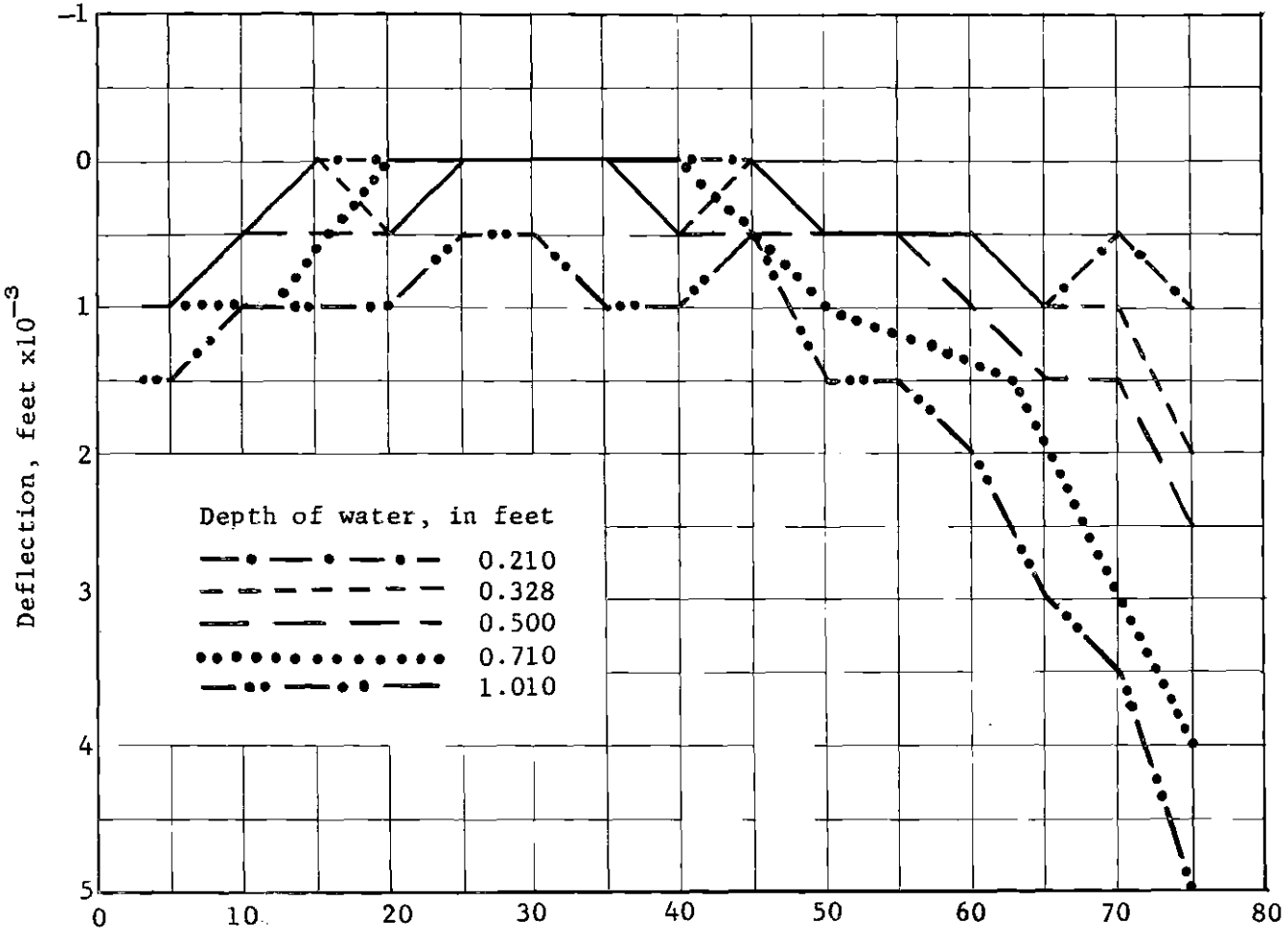

Figure 4. Flume Deflection Under Load.

openings have also been installed in the flume floor.

Water is supplied to the flume by the laboratory recirculating system through either a 12-inch or a six-inch line. Discharges are measured by a venturi meter located in the 12-inch line, or by an orifice meter located in the six-inch line. Both meters were calibrated gravimetrically.

The depth of flow in the flume is regulated by an adjustable tailgate, or by a sluice gate at the entrance of the flume.

At a later time an overbank section was placed in this flume giving a channel with a two-foot wide main flow passage and a 1.5 foot wide overbank. (See Figure 2(b).) These two sections were connected by a vertical wall 0.4 foot in height. A rectangular channel two-feet wide and 0.4 foot deep was then available.

CHAPTER III

EXPERIMENTAL PROCEDURES AND ANALYSIS

Scope of the Tests

Twenty-two tests in the 3.5-foot wide channel, which were previously collected by the U. S. Geological Survey and partially reported by Tracy and Lester (6), and four tests in the two-foot wide channel, which were also collected by the U. S. Geological Survey personnel and have not been published at this time, were used in this investigation. The pertinent information for each of these tests is listed in Table 1.

Depth Measurements

Near the normal depth, flow in uniform channels varies gradually from section to section. The change may be almost imperceptible over short distances as, for example, the 80 feet length of the experimental flume. For mild channel slopes, the normal surface-profile is the upstream asymptote to the M1 and M2 backwater curves. For steep slopes the normal profile is the downstream asymptote to the S2 and S3 curves. In each case, the normal line lies between the two curves. The method used to determine the normal flow depth consisted of the measurement of the surface profile at depths just greater than the normal, and at depth just smaller than the normal. The normal depth was then interpolated between the two curves. Point gage readings to the nearest 1/1,000th of a foot were made at five points in cross sections at one foot intervals for the length of the flume. The point-gage readings were compared with the

piezometric level at selected points in the flume.

In Figure 5 is shown a typical set of depth measurements for both a mild and a steep slope.

Table 1. Summary of Data

Test No.	B ft	U fps	y_o/B	$\gamma\, y_o S_o$ lbs/ft^2	$\mathbb{R}$
1	3.49	2.135	0.0752	0.02170	179,300
2	3.49	1.430	0.1142	0.01068	163,800
3	3.49	1.777	0.1152	0.01575	217,000
4	3.49	2.455	0.1182	0.02840	310,100
5	3.49	2.750	0.1198	0.03425	350,400
6	3.49	2.015	0.1422	0.02010	327,600
7	3.49	1.330	0.0616	0.00929	108,100
8	3.49	1.145	0.0287	0.00807	43,770
9	3.49	1.355	0.0424	0.01020	76,540
10	3.49	0.771	0.0424	0.00381	43,510
11	3.49	6.145	0.0978	0.14080	726,900
12	3.49	2.295	0.0284	0.02900	85,970
13	3.49	7.700	0.0532	0.22650	564,000
14	3.49	6.720	0.0550	0.17810	456,700
15	3.49	5.850	0.0559	0.14030	408,000
16	3.49	5.800	0.1012	0.13100	680,800
17	3.49	4.540	0.1030	0.08570	552,600
18	3.49	6.080	0.0740	0.14950	581,300
19	3.49	4.640	0.0800	0.08900	480,500
20	3.49	6.250	0.0263	0.17080	232,500
21	3.49	1.898	0.0868	0.01732	177,900
22	3.49	2.300	0.2115	0.02555	475,000
23	1.99	4.450	0.1156	0.23250	522,500
24	1.99	1.697	0.0740	0.01630	82,330
25	1.99	3.670	0.0489	0.06720	116,000
26	1.99	4.360	0.1975	0.03380	263,500

Velocity Measurements

Point velocities were measured by means of a stagnation tube connected to a manometer, with floor piezometers connected to another

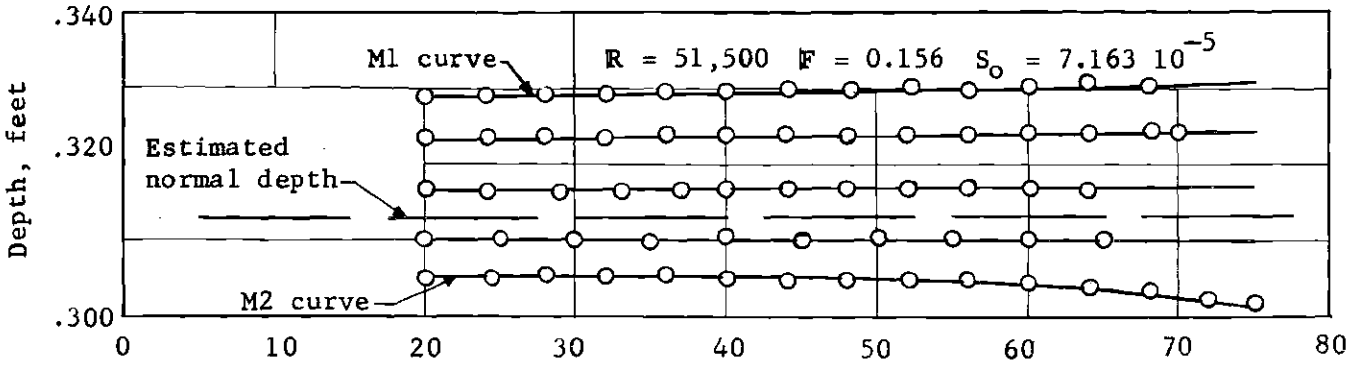

Distance along flume, feet.

(a)

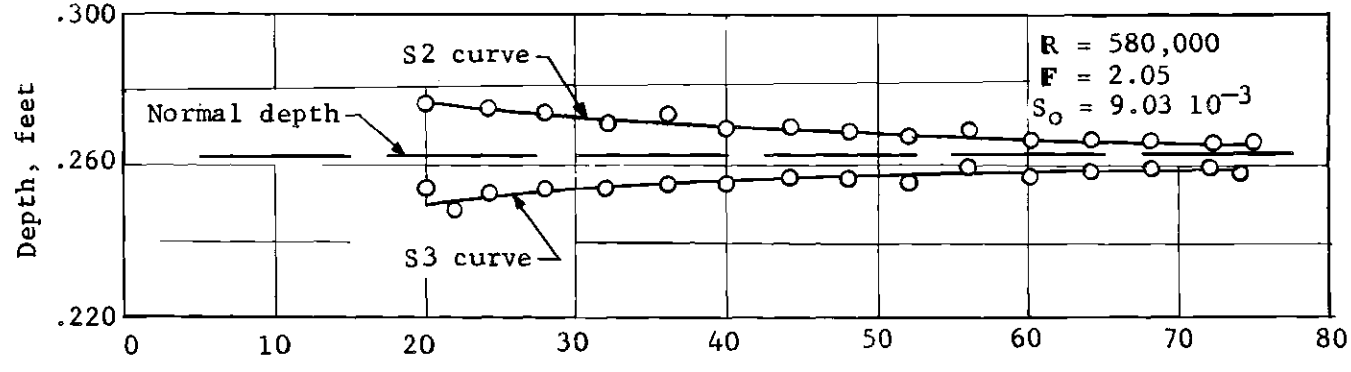

Distance along flume, feet.

(b)

Figure 5. Typical Surface Profiles

manometer. The velocity data were taken at the downstream end of the flume in the vicinity of 70 feet. The stagnation tube was held in place by an arm on a carriage, which can be rolled on the rails along the top of the sidewalls and can be locked in place anywhere along the flume. The carriage has a mechanism for precise positioning of the stagnation tube in both the horizontal and the vertical directions. The distance of the stagnation tube above the flume bottom and away from the vertical wall can be determined to the nearest 1/10,000 of a foot.

Point velocity readings were taken in vertical traverses starting near the floor, with readings taken at predetermined intervals moving towards the water surface. These traverses were taken at predetermined intervals from the channel centerline towards the wall with a traverse along the wall being taken with the stagnation tube in contact with the wall.

Shear Stress Analysis

Two methods were used in the determination of the shear stress at points along the periphery of the channel. The first method involved using Von Kármán's logarithmic law and the velocity data. Von Kármán's logarithmic law with values of the constants established from Nikuradse's experiments (11) is:

$$\frac{u}{u_*} = 5.5 + 5.75 \log \left(\frac{y u_*}{\nu}\right) \qquad (6)$$

Multiplying Equation (6) by u_* and rearranging terms,

$$u = 5.75\, u_* \log y + \left(5.75\, u_* \log \frac{u_*}{\nu} + 5.5\, u_*\right) \qquad (7)$$

from which it can be seen that 5.75 u_* is equal to the slope of the vertical velocity traverse curve when plotted as in Figure 6. Since $u_* = \sqrt{\tau_o/\rho}$, the shear stress can be determined. The second method used to determine the shear stress was Preston's method. This method was used for those tests in which the stagnation tube was placed in contact with the channel boundary. The first method was only used for the channel bottom. For the limited number of tests, data were available to make shear stress determinations by both methods. The results compare favorably.

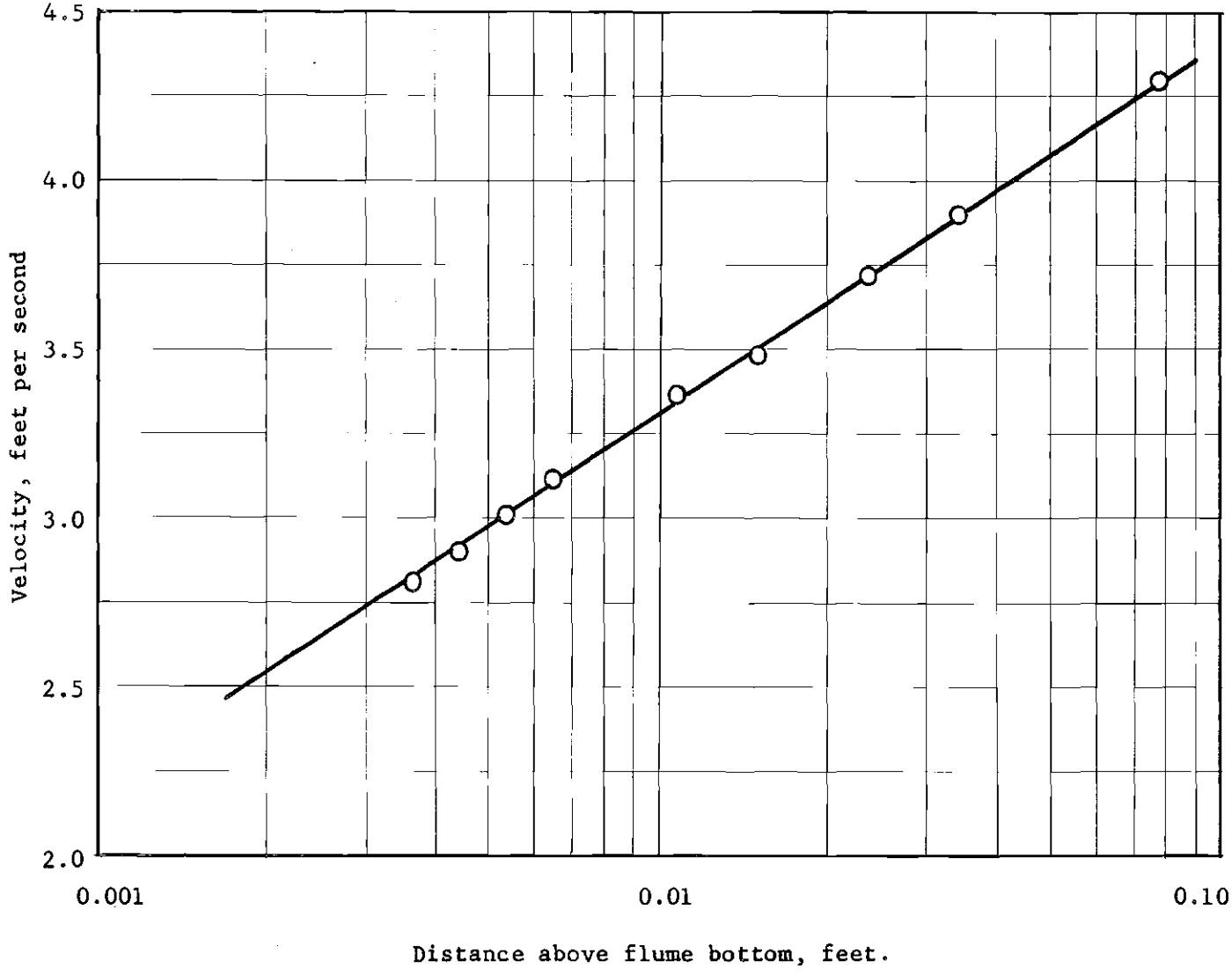

Figure 6. Typical Vertical Velocity Traverse (Central Region).

CHAPTER IV

DISCUSSION OF RESULTS

Distribution of the Shear Stress

Figures 7 through 13 are presented showing the shear stress distribution across the channel bottom. Each figure represents a different range of depth-to-width ratios. The curves were plotted with, $\tau_{ob}/\gamma\ y_o S_o$, the actual shear stress divided by the two-dimensional shear stress as a function of, $z/\frac{1}{2}B$, the ratio of the distance from the vertical wall to one-half the width of the channel.

From Figures 7 through 13 it is observed that the value of the shear stress, τ_{ob}, divided by the two-dimensional shear stress, $\gamma\ y_o S_o$, decreases as the depth-to-width ratio increases. Therefore a curve for depth-to-width ratio of 0.25 would probably be similar to Figure 13 with slightly lower values for the shear stress.

Figure 14 shows the shear stress distribution for channels with a depth-to-width ratio of 0.25 and 0.50 as presented by Lane (7). Comparing Figure 14 with Figure 13 it is observed that Lane's mathematically described distribution is of a considerably different nature than that described by the writer's data. Lane's distribution has values in the center of the channel that are higher than those determined from the writer's analysis.

The shear stress distribution for the vertical walls, for different ranges of depth-to-width ratios, are shown on Figures 15 through 19. The

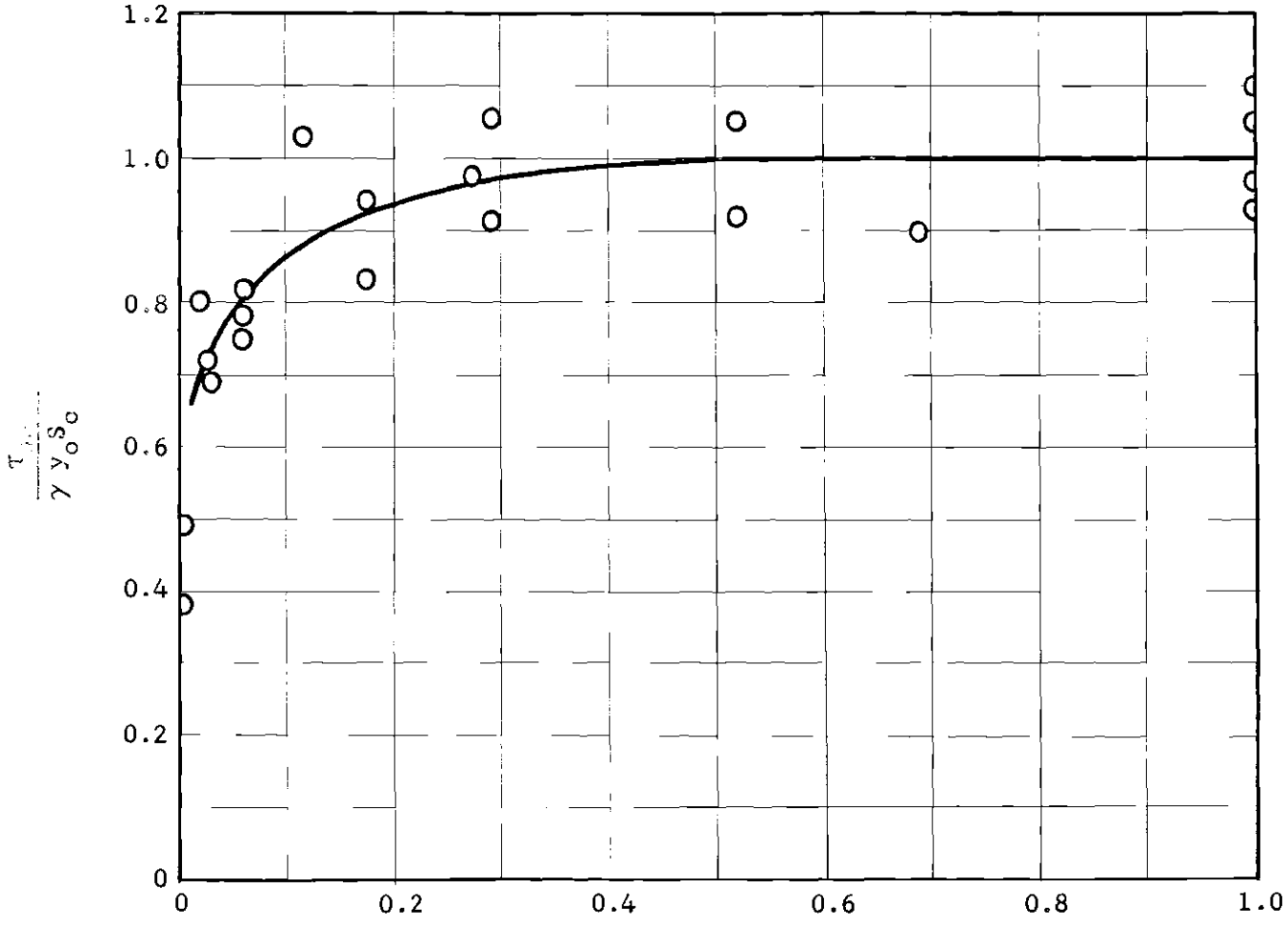

Figure 7. Shear Stress Distribution, Bottom, ($0.026 < y_o/B < 0.030$).

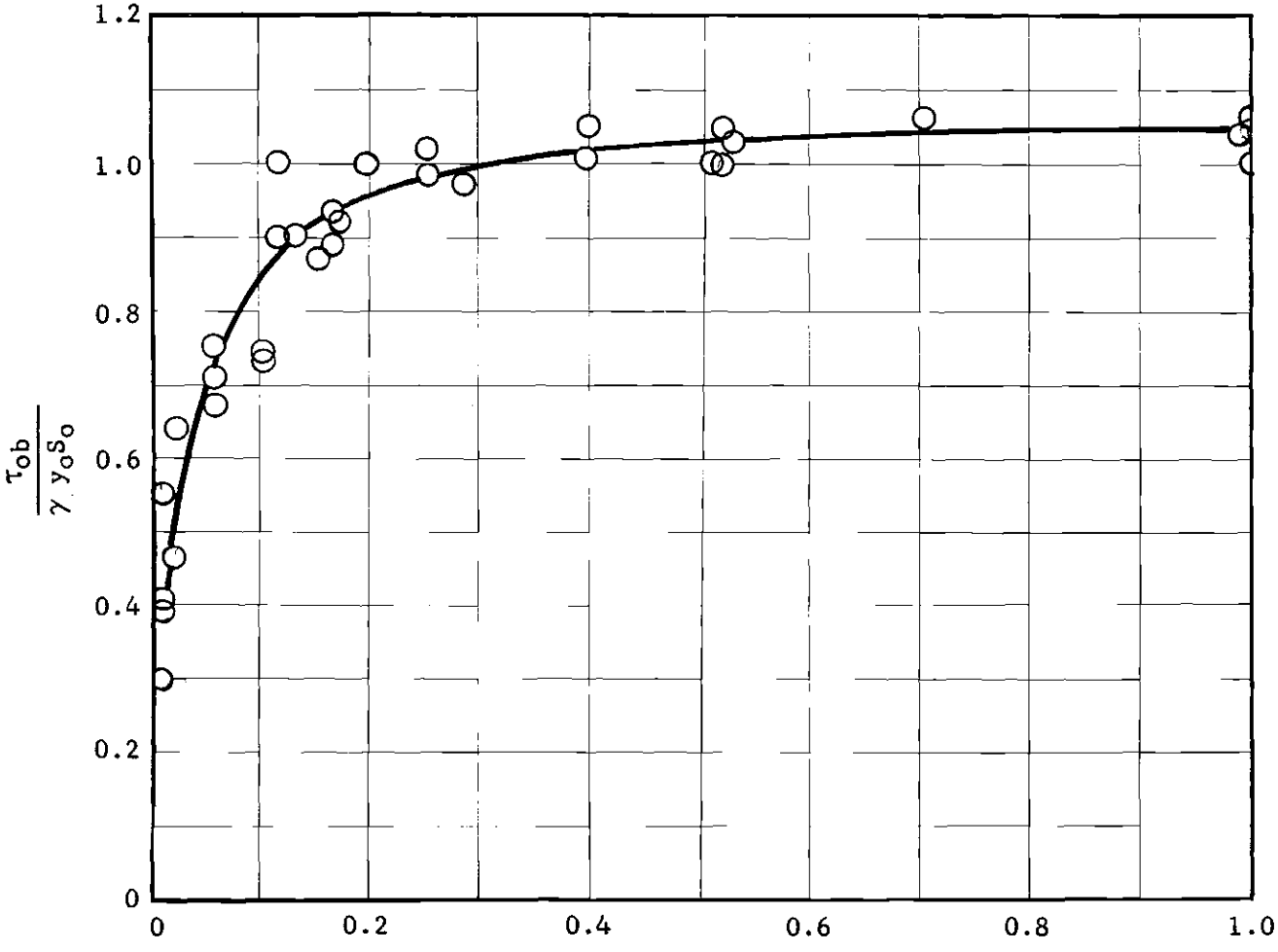

Figure 8. Shear Stress Distribution, Bottom, ($0.040 < y_o/B < 0.050$).

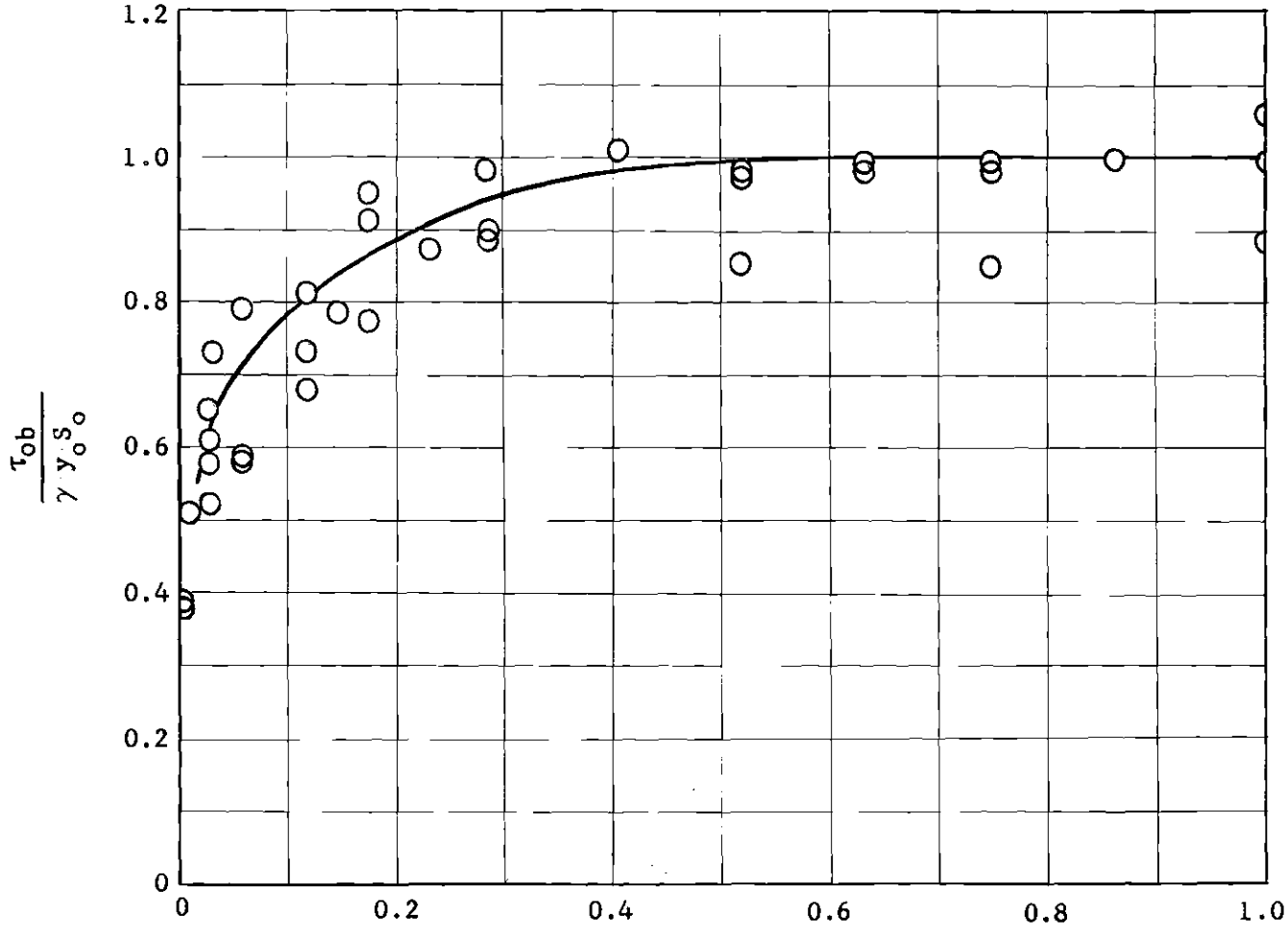

Figure 9. Shear Stress Distribution, Bottom, $(0.050 < y_o/B < 0.062)$.

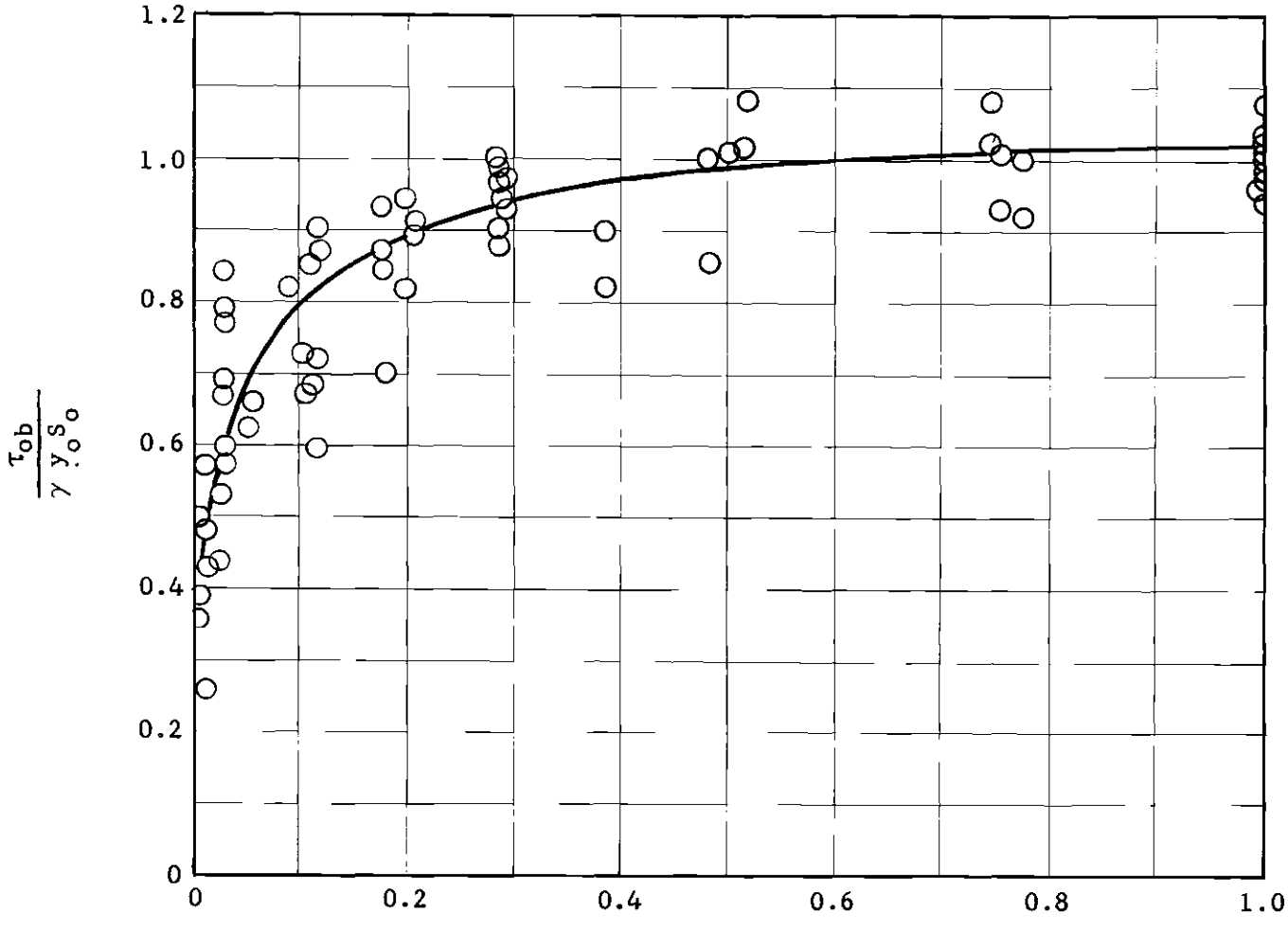

Figure 10. Shear Stress Distribution, Bottom, ($0.074 < y_o/B < 0.087$).

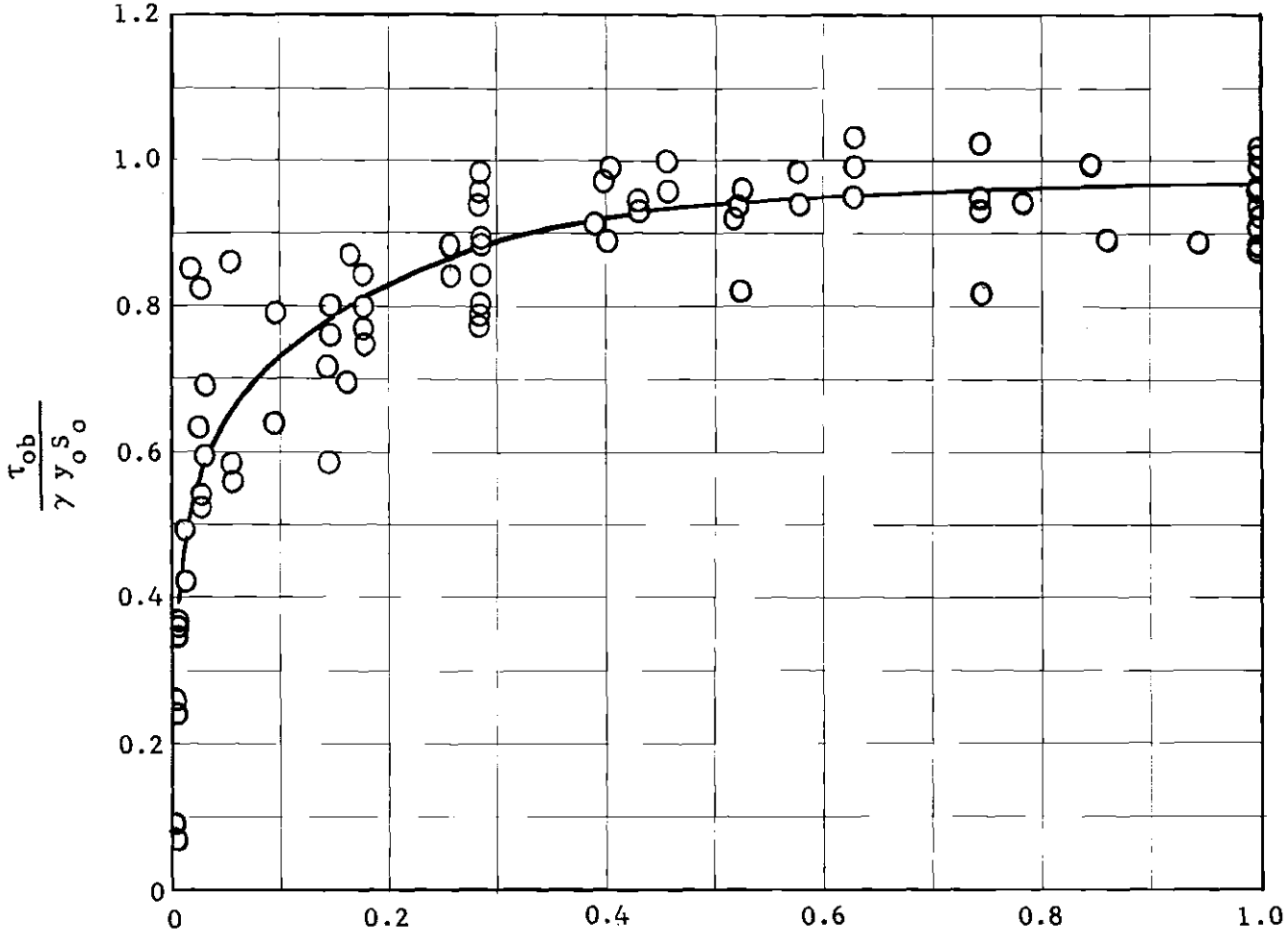

Figure 11. Shear Stress Distribution, Bottom, ($0.110 < y_o/B < 0.120$).

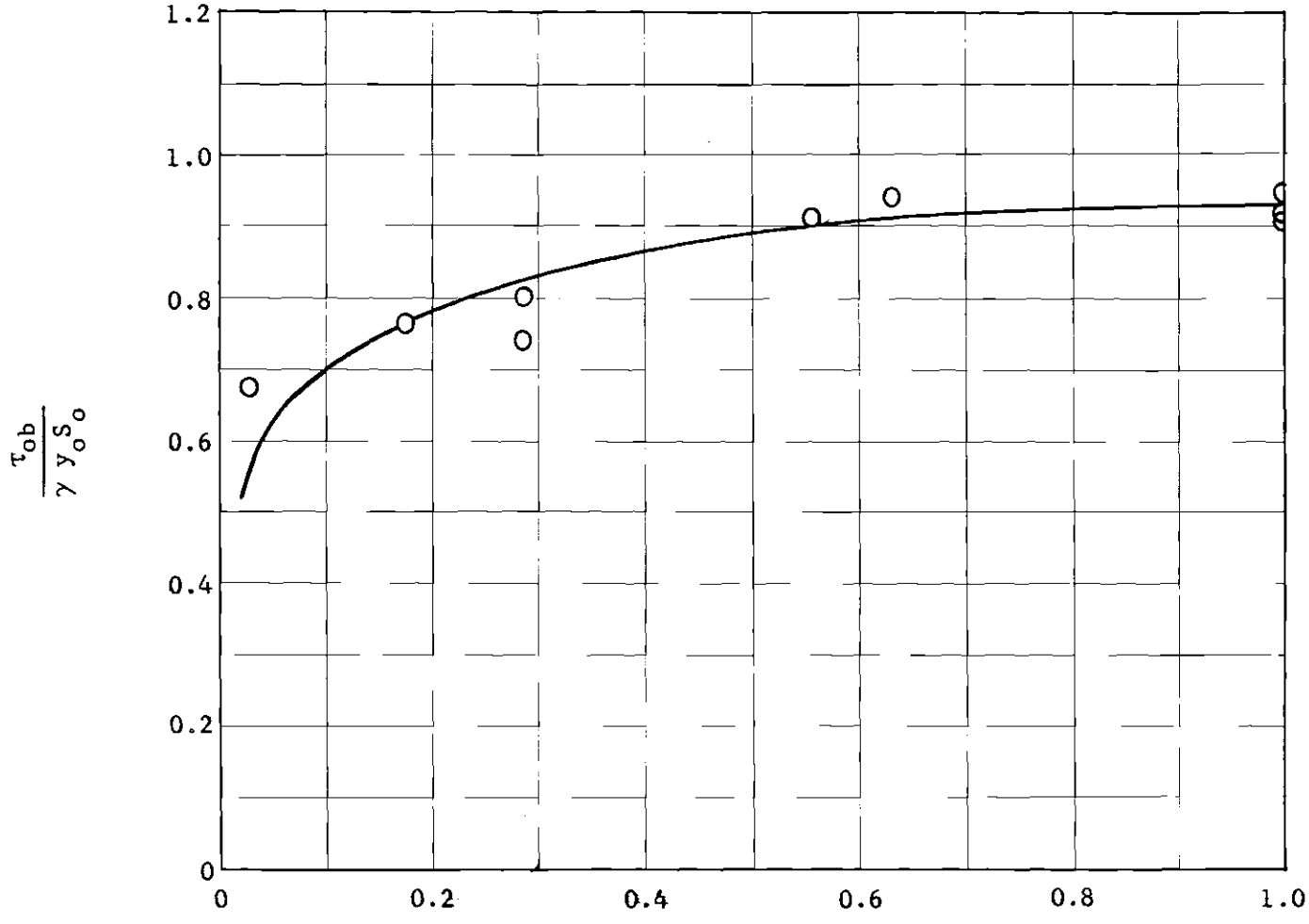

Figure 12. Shear Stress Distribution, Bottom, ($0.140 < y_o/B < 0.145$).

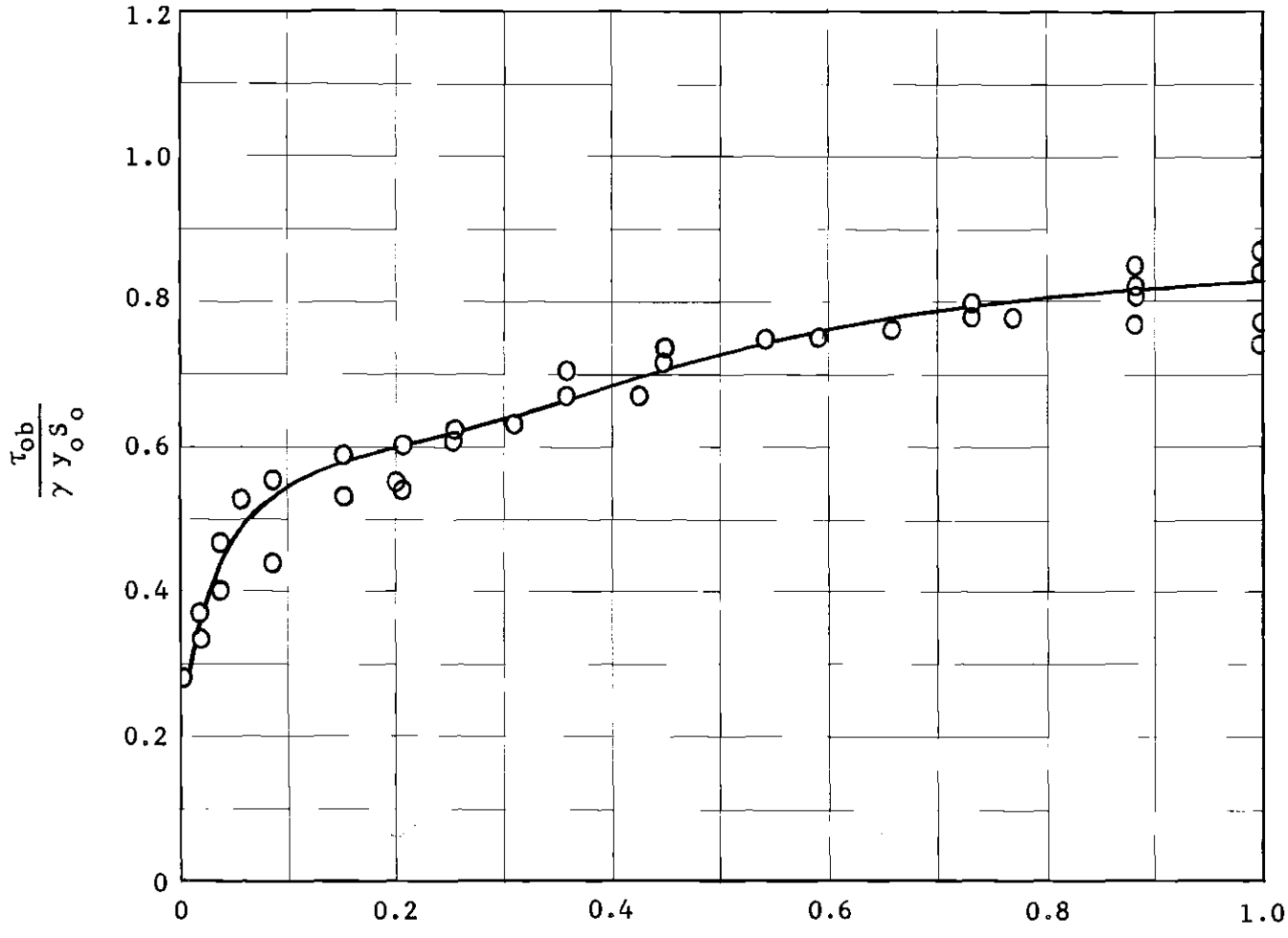

Figure 13. Shear Stress Distribution, Bottom, ($0.195 < y_o/B < 0.215$).

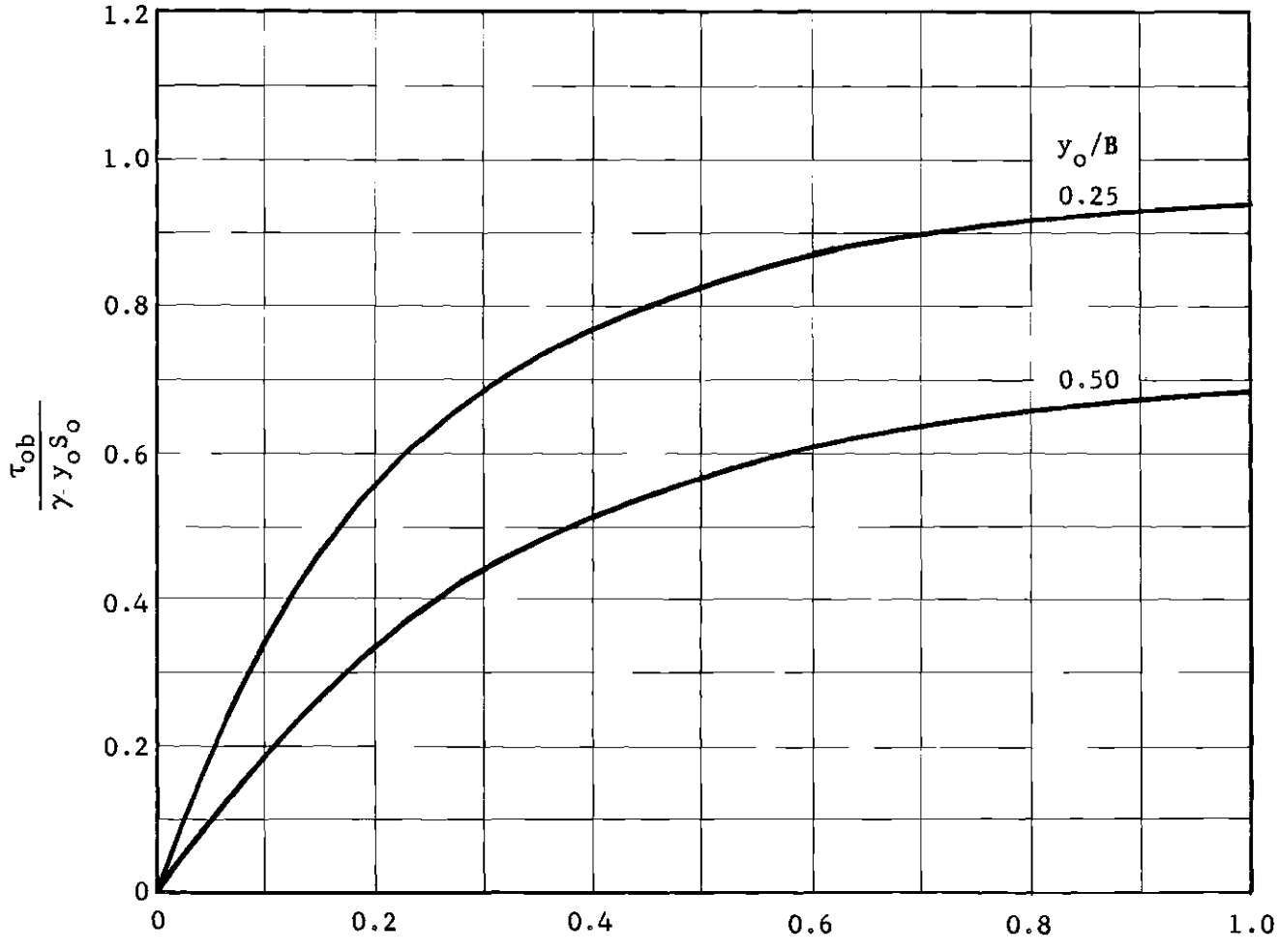

Figure 14. Shear Stress Distribution, Bottom, (Lane (7)).

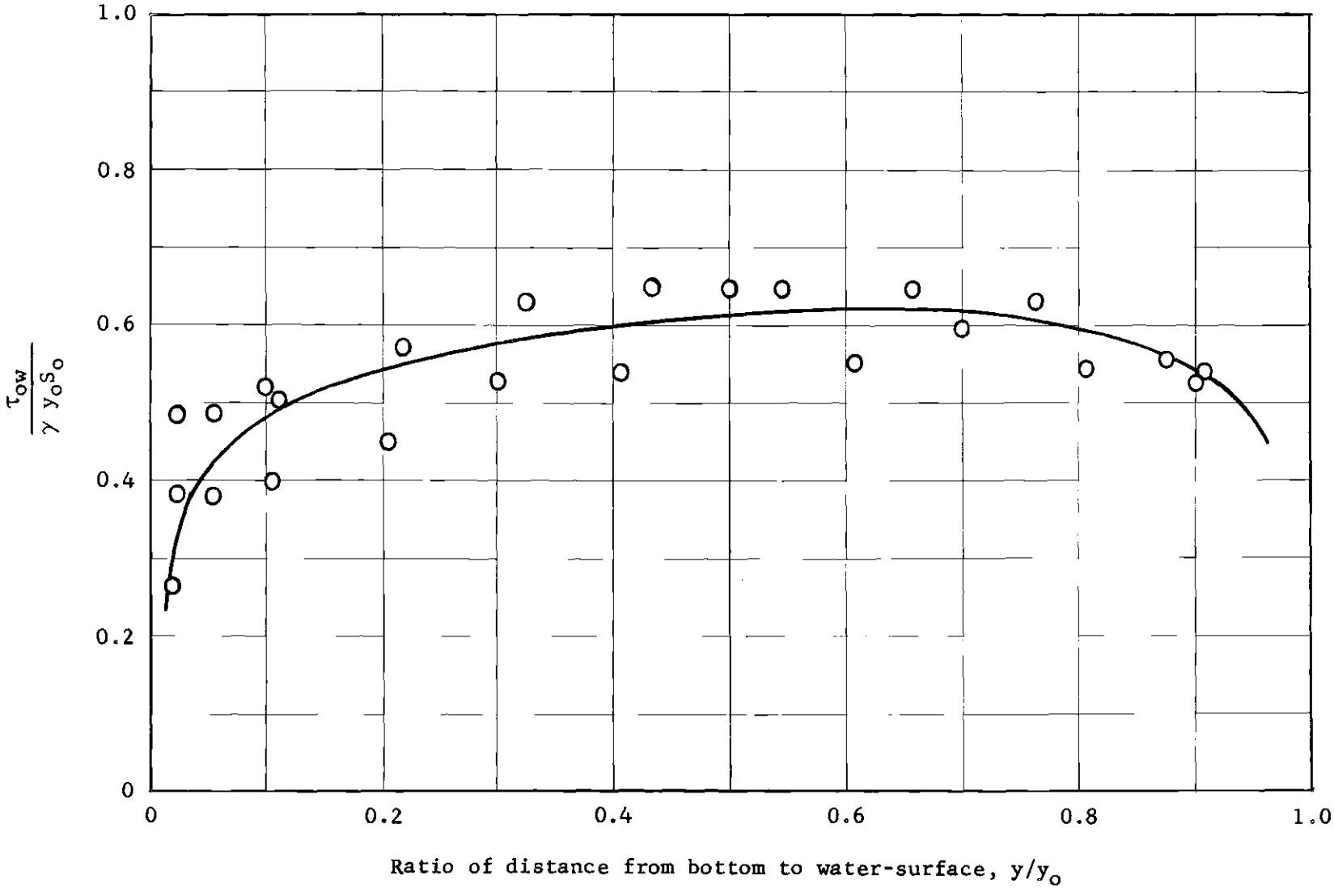

Figure 15. Shear Stress Distribution, Wall, ($0.026 < y_o/B < 0.030$).

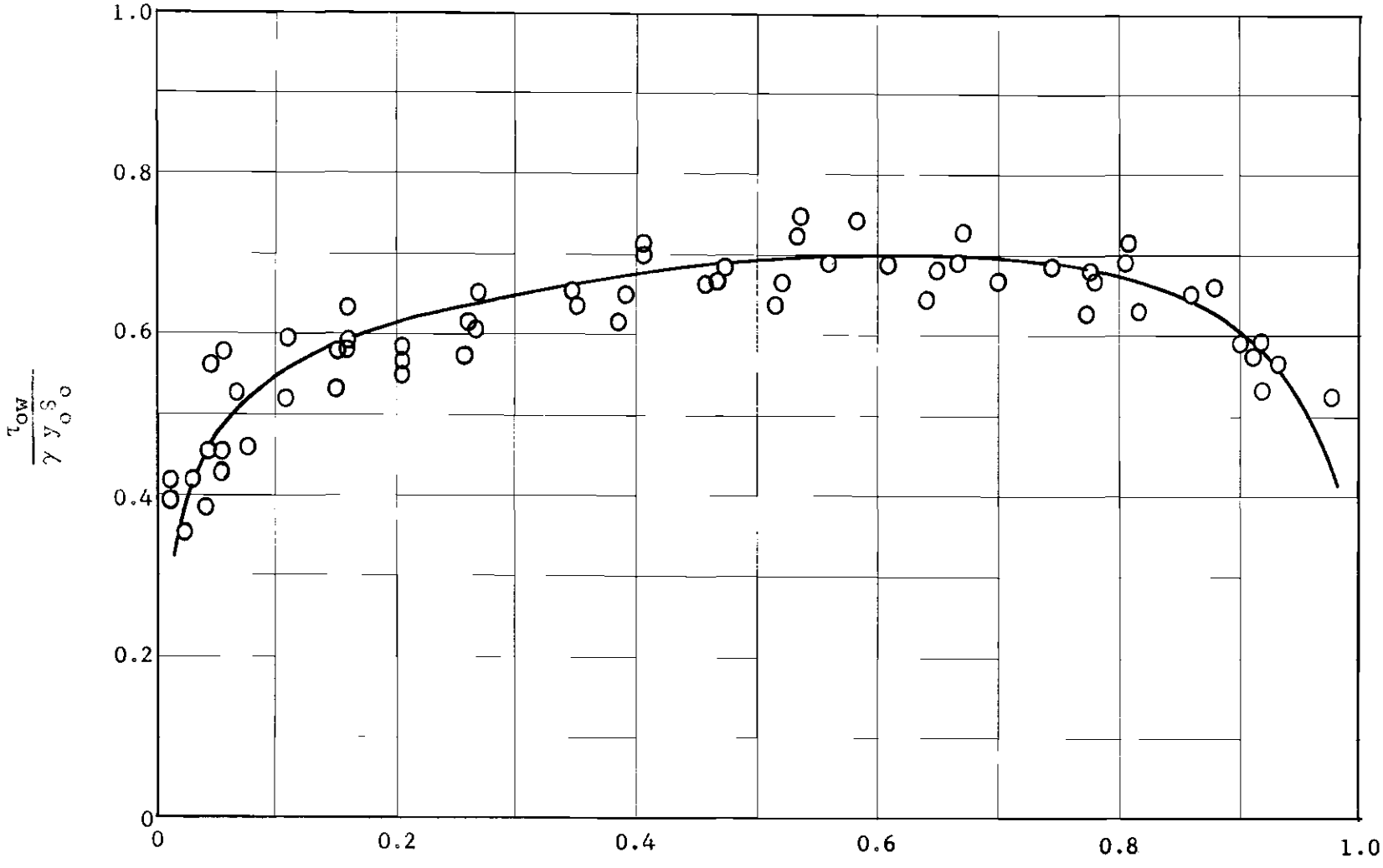

Figure 16. Shear Stress Distribution, Wall, ($0.040 < y_o/B < 0.062$).

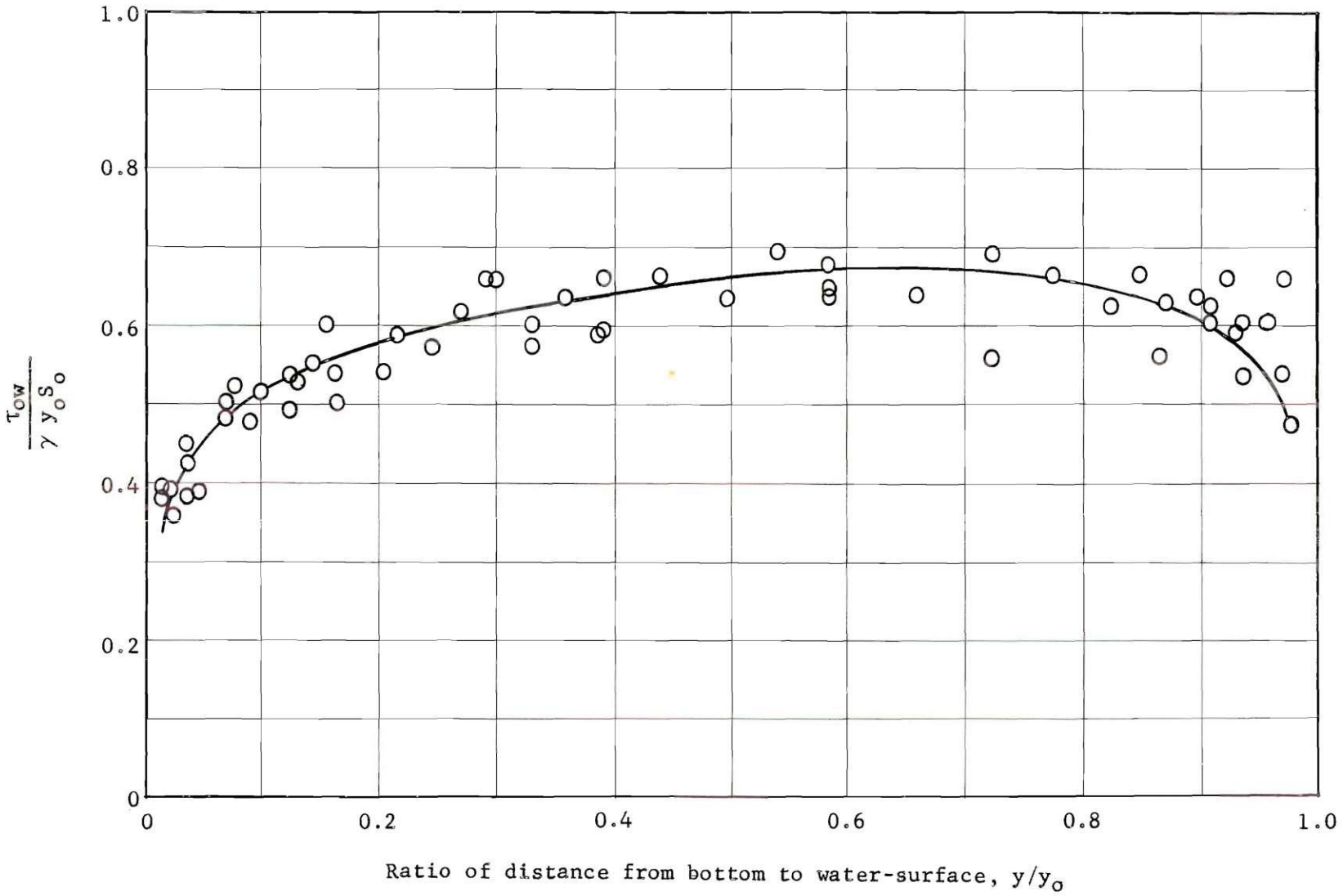

Figure 17. Shear Stress Distribution, Wall, ($0.074 < y_o/B < 0.087$).

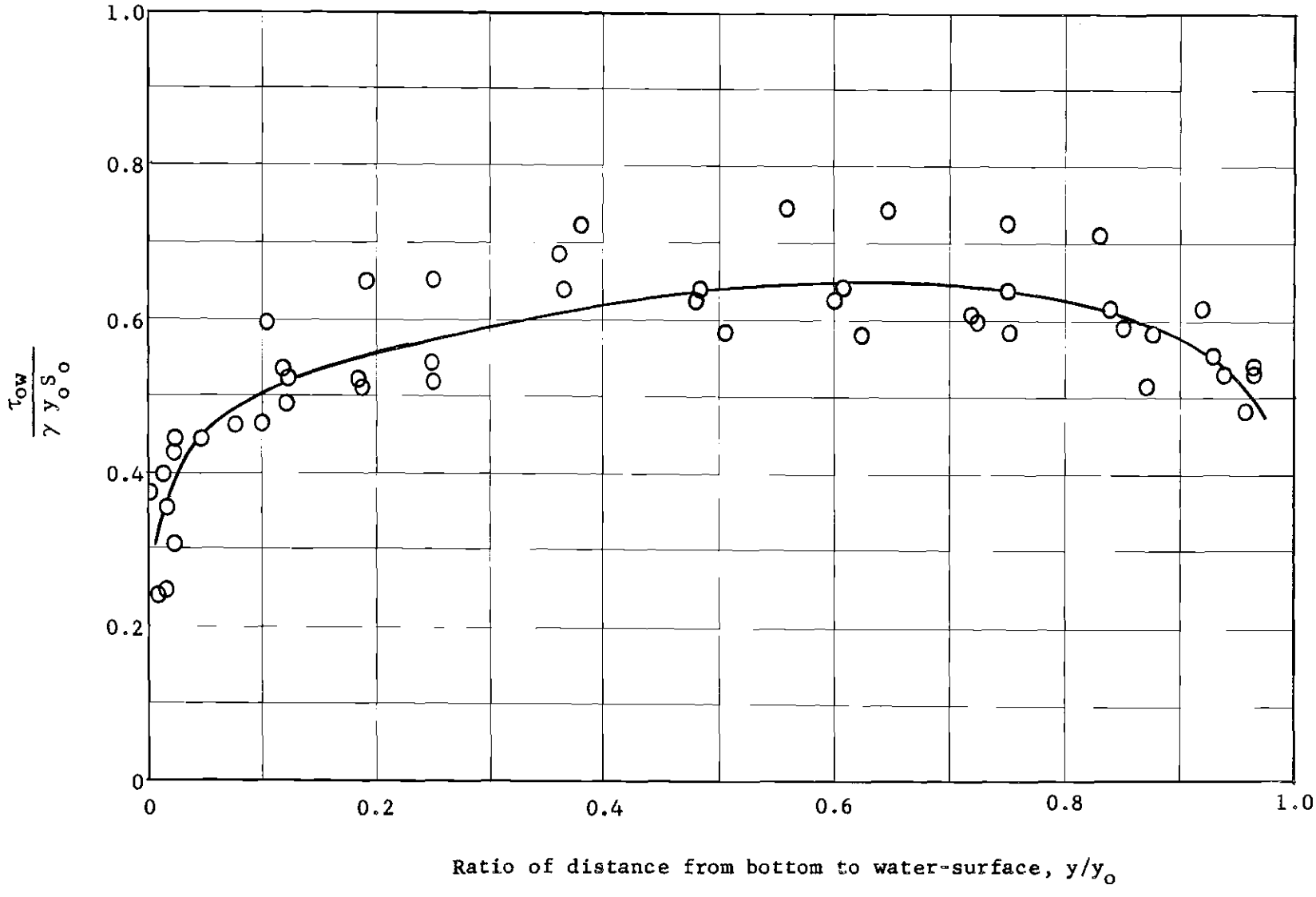

Figure 18. Shear Stress Distribution, Wall, ($0.110 < y_o/B < 0.120$).

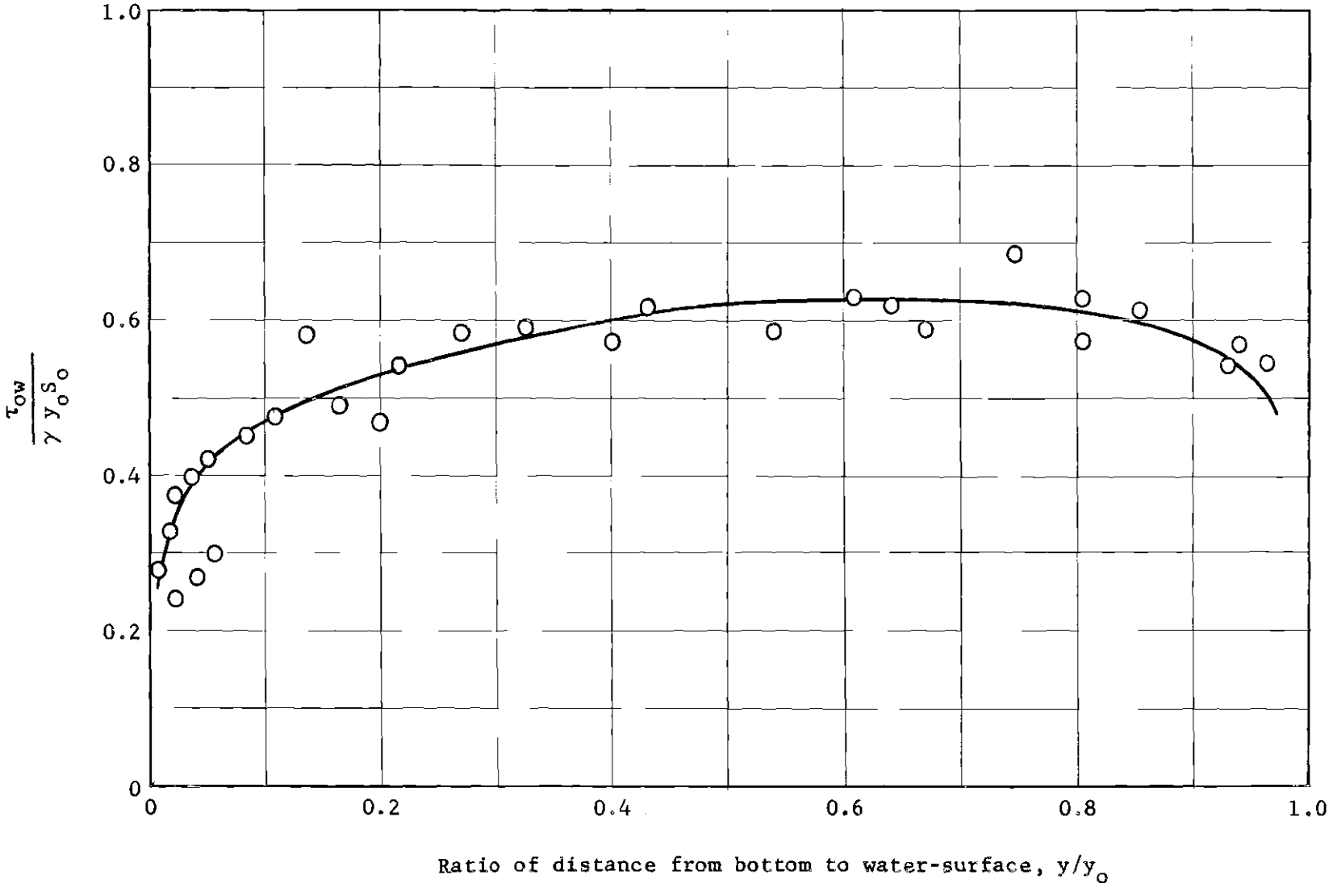

Figure 19. Shear Stress Distribution, Wall, ($0.140 < y_o/B$ 0.215).

curves are plotted with, $\tau_{ow}/\gamma\ y_o S_o$, the actual shear stress divided by the two-dimensional shear stress as a function of, y/y_o, the ratio of the distance above the channel bottom to the total flow depth.

Maximum Shear Stress

Figure 20 shows the maximum shear stress for the channel bottom, $\tau_{ob}(max.)$, divided by the two-dimensional shear stress, $\gamma\ y_o S_o$, as a function of the depth-to-width ratio of the channel cross-section. The values of maximum shear stresses shown in Figure 20 were obtained from Figures 7 through 13 at $z/\frac{1}{2}B = 1.0$.

If the flow were two-dimensional the maximum shear stress, $\tau_{ob}(max.)$, would be equal to $\gamma\ y_o S_o$. From Figure 20 one observes that the maximum shear stress, $\tau_{ob}(max.)$, is equal to $\gamma\ y_o S_o$ for values of y_o/B less than 0.08. The implication is that if the channel is narrower than the limit $y_o/B = 0.08$, no two-dimensional flow zone exists. In other words, the width of the region affected by the wall is about six times the flow depth.

Tracy and Lester (5) report that, for the velocity distribution, the width of the wall region is two-to-three times the flow depth. They define the wall region as that region which lies between the vertical wall and the vertical velocity traverse which first deviates from the characteristic logarithmic profile of the central region.

The two-dimensional, central, flow region defined by the shear stress distributions is lesser in extent than that obtained using the criterion of Tracy and Lester. A reasonable assumption is that no two-dimensional flow zone exists in a rectangular channel but that the flow is approximately two-dimensional in the central regions of channels in

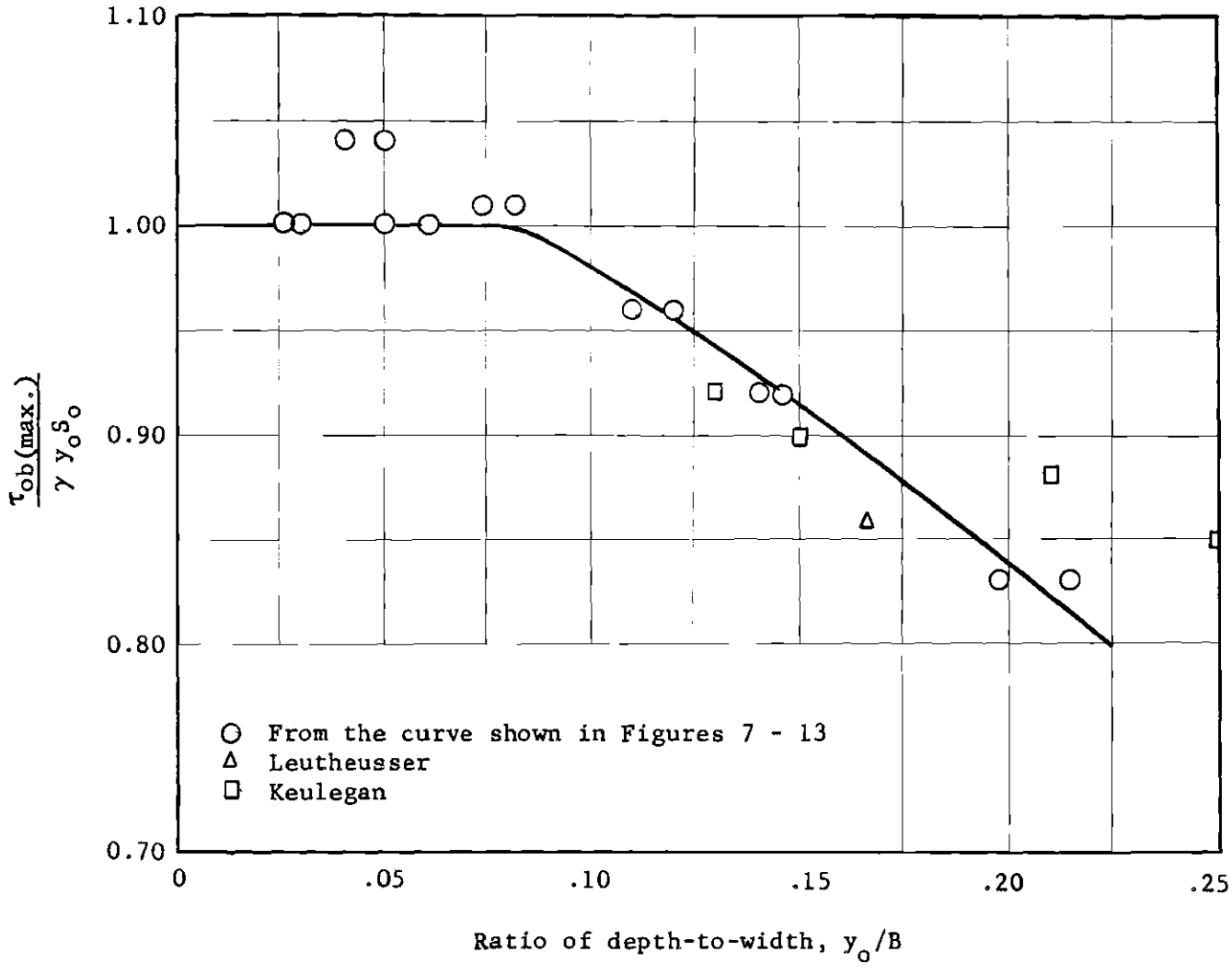

Figure 20. Maximum Shear Stress, Bottom

which $y_o/B < 0.08$. Another criterion such as the equality of turbulence characteristics would probably result in a third definition of a two-dimensional flow region.

Lane (7) derived a curve, similar to that of Figure 20, for the maximum shear stress on the channel bottom. Figure 21 is a comparison of the curve devised by Lane with the curve from Figure 20, where the curve from Figure 20 is extended to $y_o/B = 0.25$. Comparing the two curves at $y_o/B = 0.25$ it is seen that the maximum shear stresses of Lane are considerably higher than those computed from experimental measurements.

Figure 22 is a curve for the maximum shear stress on the walls, and Figure 23 shows a curve which was derived by Lane for the maximum shear stress on the wall compared with the curve from Figure 22. From Figure 23 it is observed that the maximum shear stress on the wall, computed from experimental data, is less than that given by Lane.

Average Shear Stress

The average shear stress for the bottom and for the walls was found by integrating the shear stress distribution curves for each test. Using these average shear stresses, $\bar{\tau}_o$, divided by the two-dimensional shear stress, $\gamma\, y_o\, S_o$, they were plotted in Figure 24 as a function of the depth-to-width ratio, y_o/B, of the channel cross-section. A curve for the average shear stress, for the total boundary of the cross-section, Equation (3a), is also plotted on Figure 24. An average curve was drawn through the data for the channel bottom. Then a curve for the average shear stress on the wall was computed by means of Equation (8). Equation (8) is obtained by eliminating $\gamma\, S_o$ from Equations (3) and (3a).

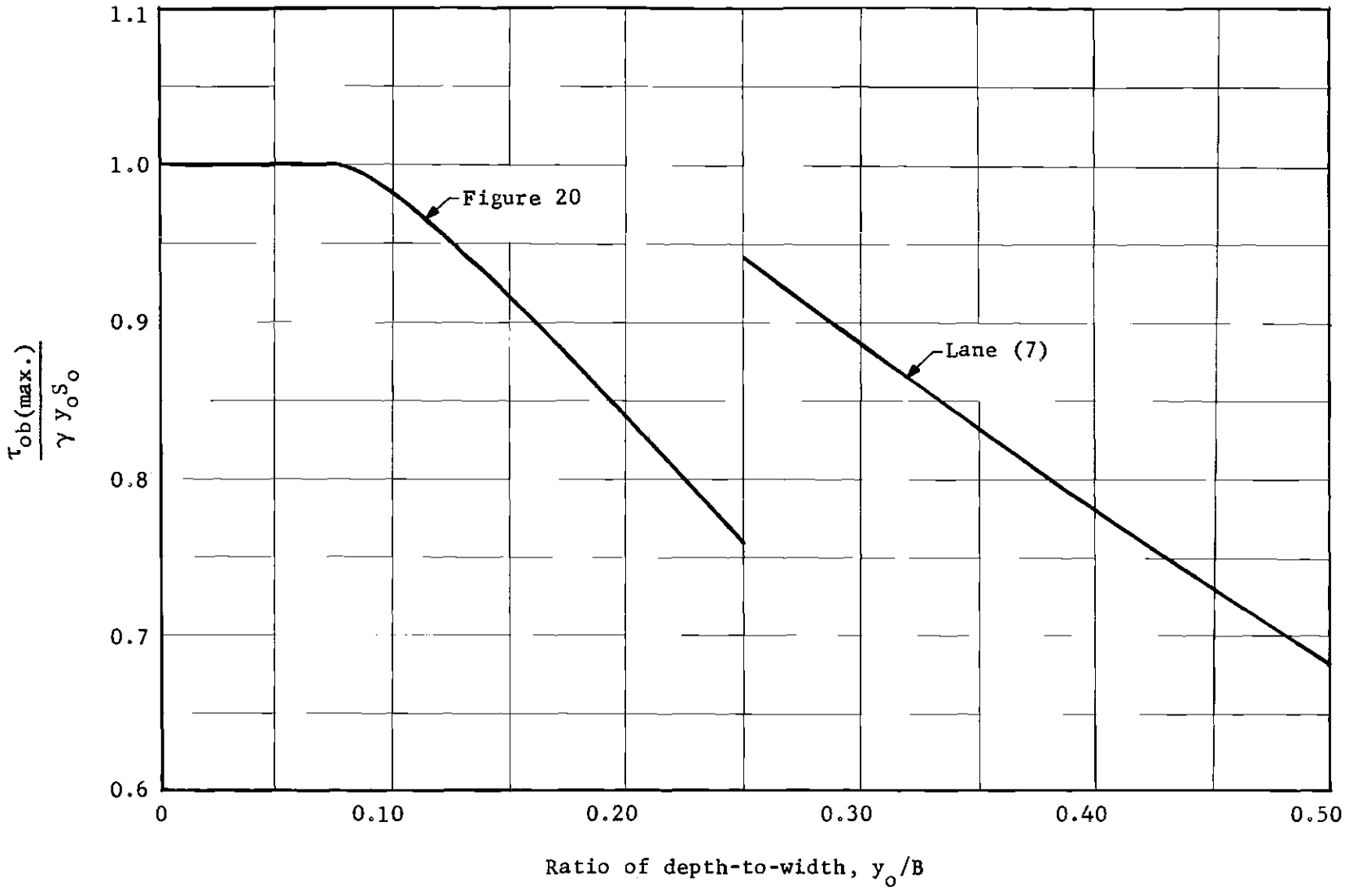

Figure 21. Maximum Shear Stress, Bottom

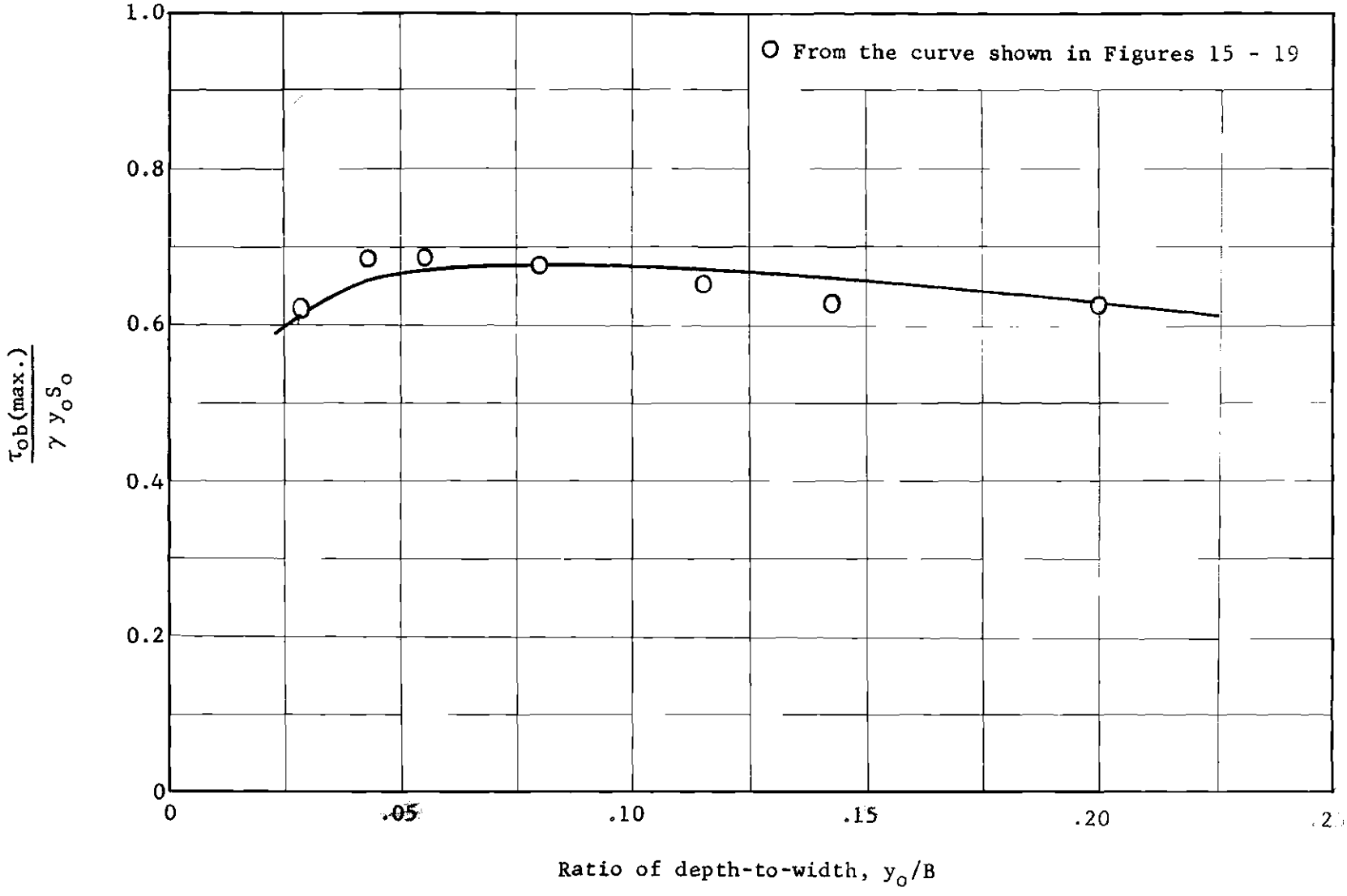

Figure 22. Maximum Shear Stress, Wall.

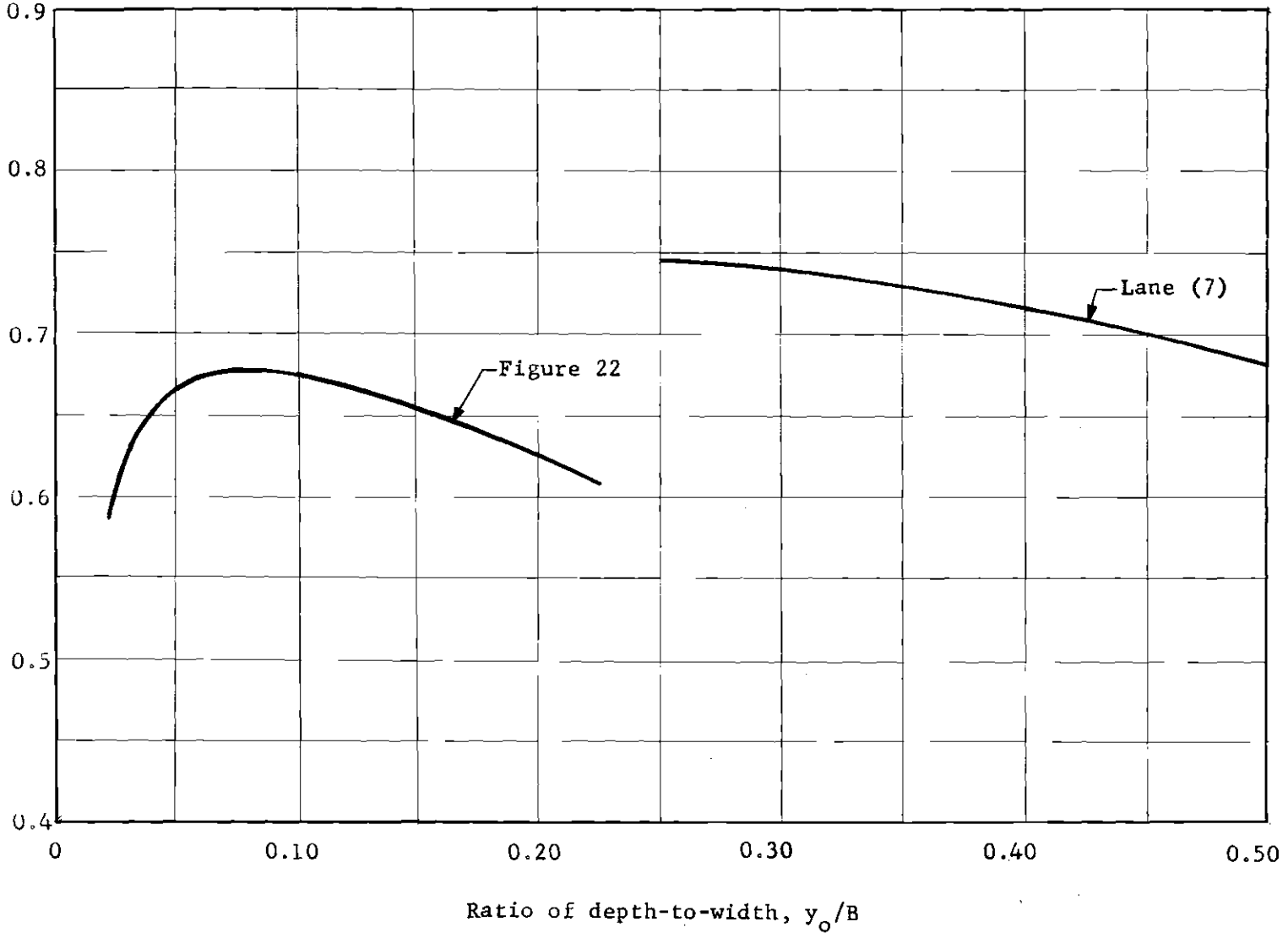

Figure 23. Maximum Shear Stress, Wall.

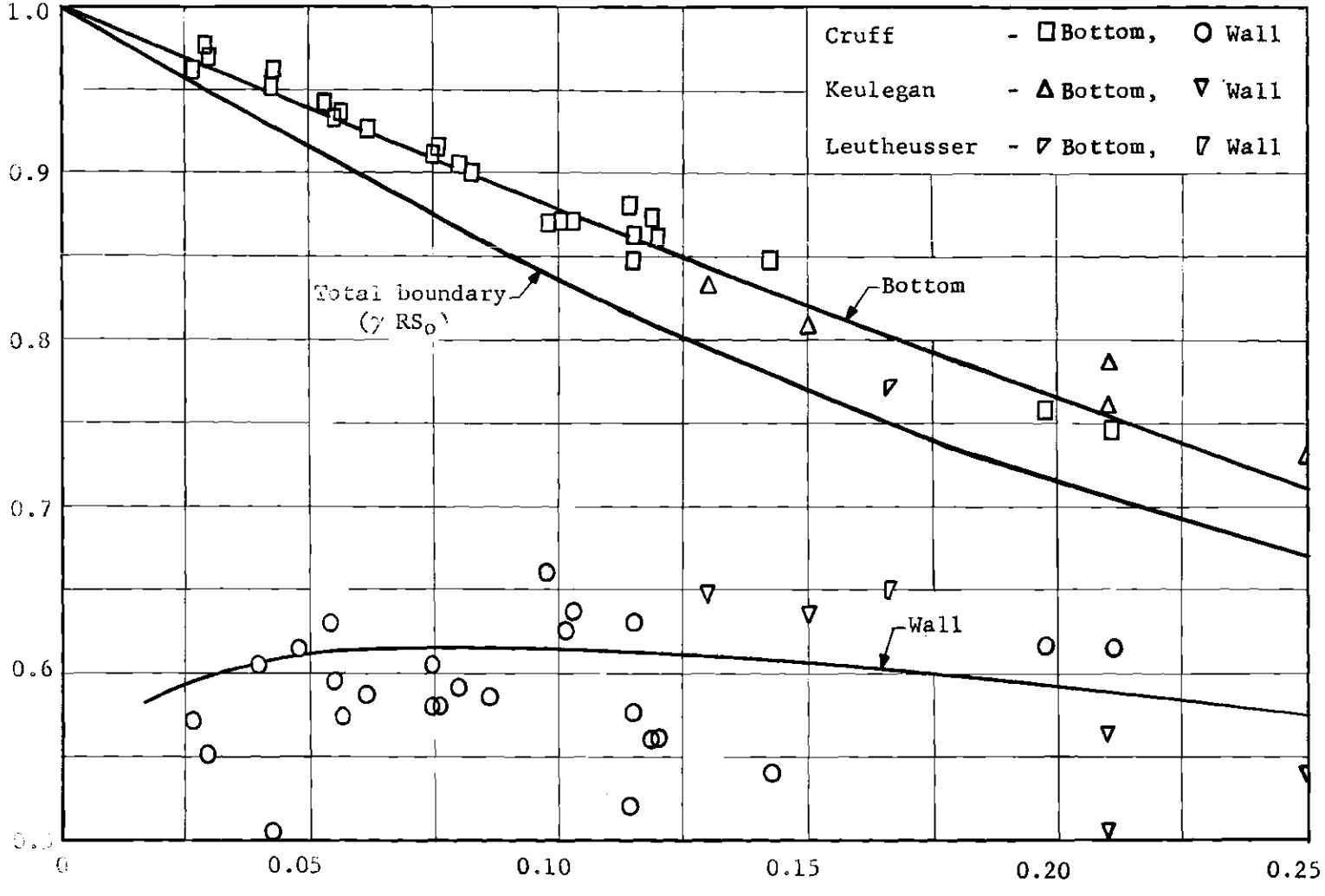

Figure 24. Average Shear Stress

$$(B + 2y_o)\ \bar{\tau}_o = (B)\bar{\tau}_{ob} + (2y_o)\bar{\tau}_{ow} \qquad (8)$$

The computed curve for the wall was found to fit the average of the wall data very well as is seen on Figure 24. An average shear stress was found from the shear stress distributions given by Keulegan (6) and Leutheusser (8). These values are also shown in Figure 24.

Apparent Shear Force

From Equation (2)

$$-\,dx\int_{\frac{1}{2}B}^{z} \tau_{ob}(-\,dz) - \bar{\tau}_a\ y_o\ dx + \gamma[(\tfrac{1}{2}B) - z](y_o \sin\theta)dx = 0 \qquad (2)$$

F_a', the apparent shear force for an incremental distance, dx, in the longitudinal direction, can be solved for by dividing Equation (2) by dx and rearranging terms. Giving the equation:

$$F_a' = y_o\ \bar{\tau}_a = \gamma[(\tfrac{1}{2}B) - z](y_o \sin\theta) - \int_{\frac{1}{2}B}^{z} \tau_{ob}(-\,dz) \qquad (9)$$

The apparent shear force for an incremental distance, dx, was computed for the tests, for various distances from the wall towards the channel centerline using Equation (9). The uniform flow slope, S_o, was substituted for sin θ. The shear stress across the channel bottom, τ_{ob}, was found from Figures 7 through 13. The fluid specific weight, γ, the uniform flow depth, y_o, the channel width, B, and the uniform flow slope, S_o, were available, from the experimental data, for each test. Figure 25 shows the values of F_a', the apparent shear force for an incremental distance, dx, divided by $\frac{1}{2}B\ \gamma\ y_o S_o$ as a function of the channel depth-to-width ratio, y_o/B, and of the ratio of the distance from the wall to the

channel centerline, $z/\frac{1}{2}B$.

Cross-Channel Transfer of Momentum

The cross-channel transfer of momentum, which was previously shown to be the apparent shear force, $\bar{\tau}_a \, y_o \, dx$, can be found for uniform flow in a smooth rectangular open channel for any section between the wall and the channel centerline. This transfer for an incremental distance, dx, can be found from Figure 26 if the fluid specific weight, γ, the uniform flow depth, y_o, the uniform flow slope, S_o, and the channel width, B, are known.

Figure 26, which was derived from Figure 25, shows curves for various depth-to-width ratios, y_o/B, of F'_a, the apparent shear force for an incremental distance, dx, divided by $\frac{1}{2}B \, \gamma \, y_o S_o$ as a function of the ratio of the distance from the wall to the channel centerline, $z/\frac{1}{2}B$.

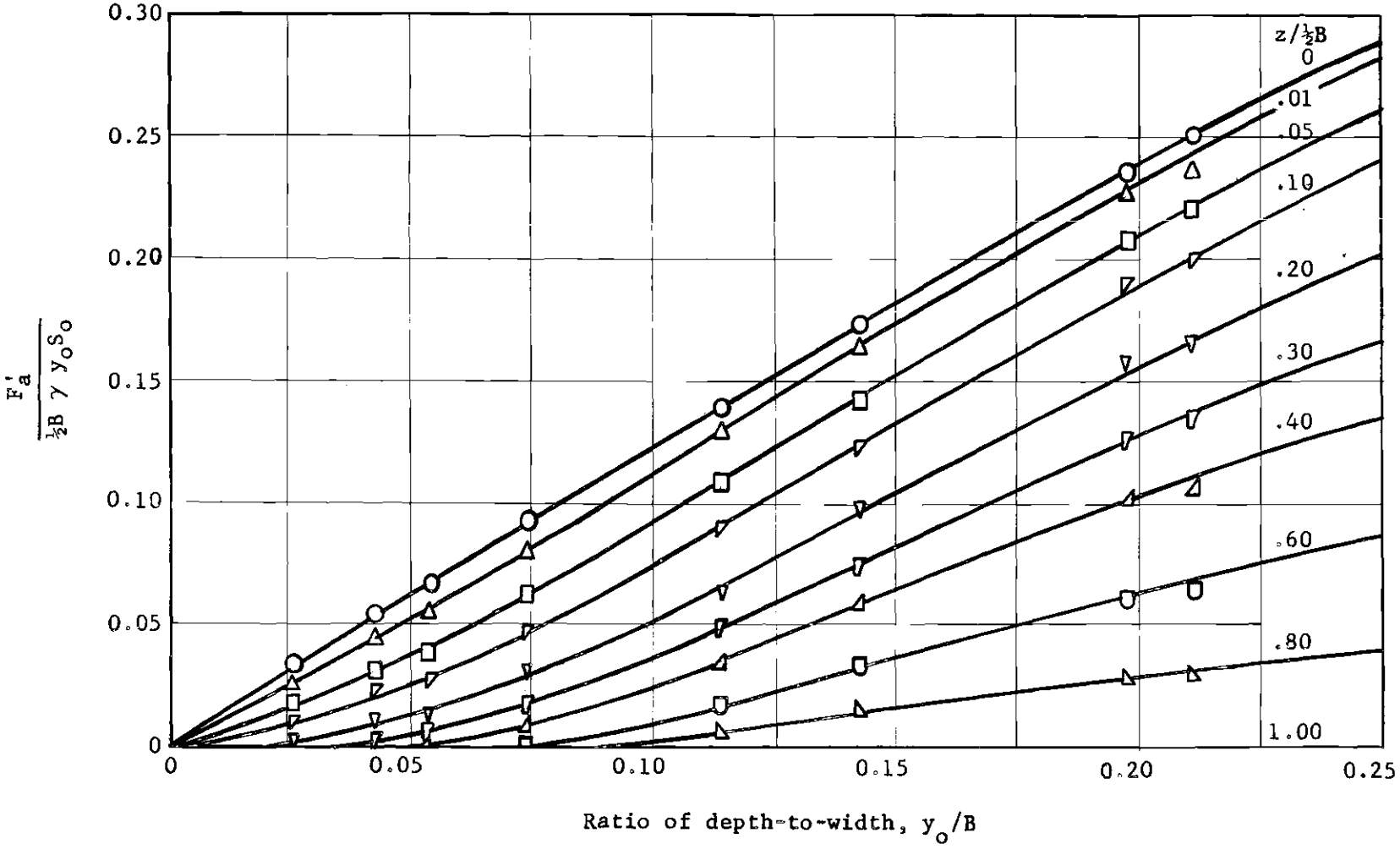

Figure 25. Apparent Shear Force

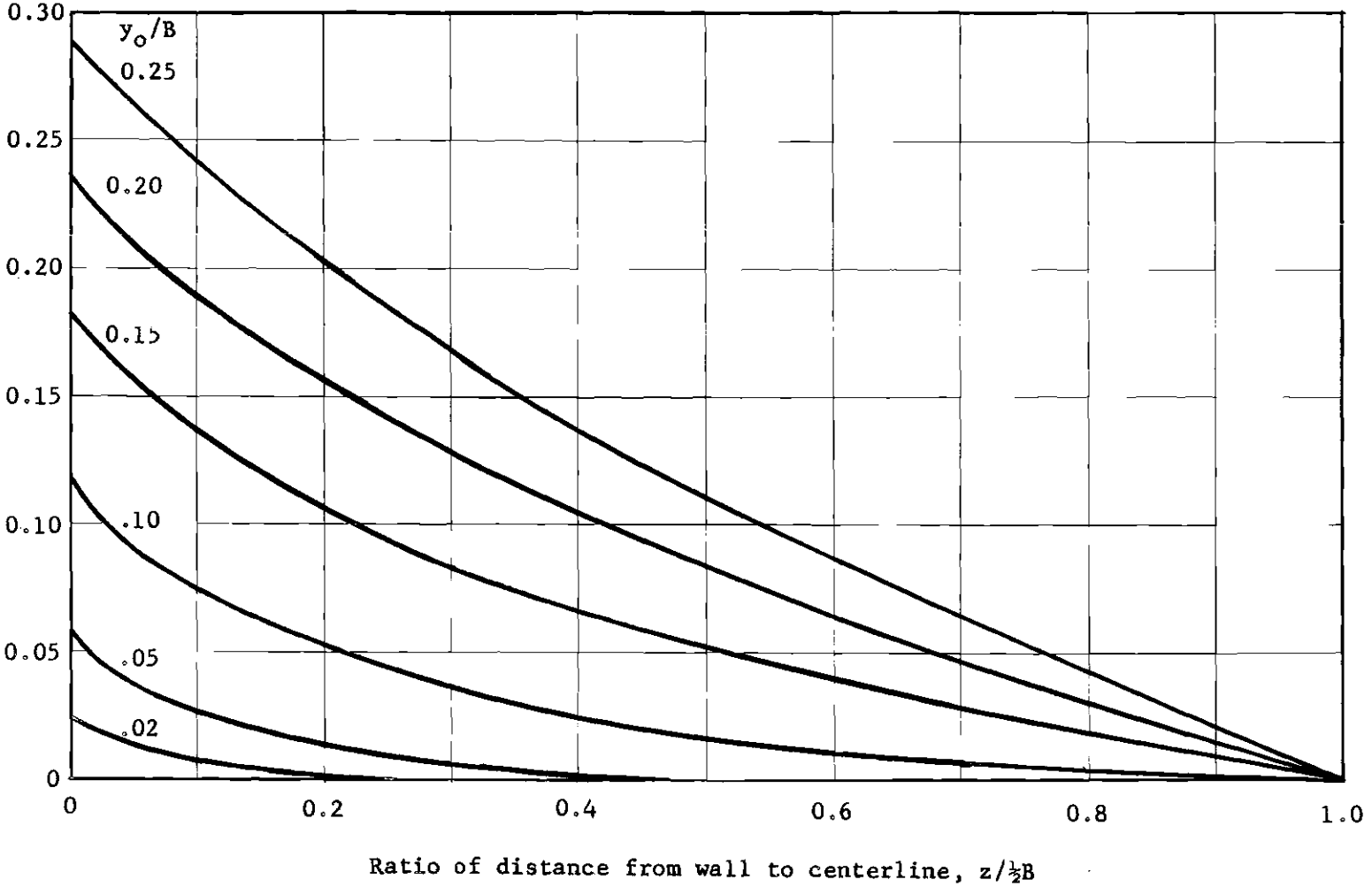

Figure 26. Apparent Shear Force

CHAPTER V

CONCLUSIONS

The study of cross-channel transfer of linear momentum is based upon data (26 tests) previously collected by the U. S. Geological Survey. The range of test conditions included depth-to-width ratios from 0.026 to 0.211, Reynolds numbers from 43,770 to 726,900, two-dimensional shear stress from 0.0038 to 0.2325 pounds per square foot, and average channel velocity from 0.77 to 7.70 feet per second.

1. The depth-to-width ratio is the only parameter affecting the shear stress distribution in a smooth rectangular open channel when the shear stress is used as a ratio of its two-dimensional shear stress.

2. There is a central flow region for which the shear stress is two-dimensional for smooth rectangular open channels with depth-to-width ratios less than 0.08. In other words, the wall affects the shear stress for a distance of about six times the flow depth, laterally from the wall towards the center of the channel.

3. The average shear stress for the channel bottom is much larger than for the channel wall at the small depth-to-width ratios, with this difference becoming less at the larger depth-to-width ratios.

BIBLIOGRAPHY

1. Wilroy, R. D., An Investigation of the Critical Depth in an Open Channel with a Nonrectangular Cross Section, Unpublished M. S. Thesis, Georgia Institute of Technology, 1953.

2. Rodriguez-Diaz, A. J., The Hydraulic Jump in a Non-Rectangular Open Channel, Unpublished M. S. Thesis, Georgia Institute of Technology, 1954.

3. Prandtl, L., Fluid Dynamics, Hefner Publishing Co., New York, 1952, p. 148-149, (Translation by W. M. Deans).

4. Laufer, John, "Investigation of Turbulent Flow in a Two-Dimensional Channel," National Advisory Committee for Aeronautics, TR-1053, 1951.

5. Tracy, H. J., and Lester, C. M., "Resistance Coefficients and Velocity Distribution-Smooth Rectangular Channel," Water Supply Paper 1592A, U. S. Department of the Interior, Geological Survey, 1961, 18 p.

6. Keulegan, G. H., "Laws of Turbulent Flow in Open Channels," Journal of Research, National Bureau of Standards, vol. 21, December 1938, pp. 707-741.

7. Lane, E. W., "Design of Stable Channels," Transactions, American Society of Civil Engineers, vol. 120, 1955, pp. 1234-1279.

8. Leutheusser, H. J., "Turbulent Flow in Rectangular Ducts," Journal of the Hydraulics Division, American Society of Civil Engineers, vol. 89, No. HY3, May 1963, pp. 1-19.

9. Hsu, E. Y., The Measurement of Local Turbulent Skin Friction by Means of Surface Pitot Tubes, U. S. Navy Department, Taylor Model Basin, Research and Development Report 957, August 1955, 18 p.

10. Hwang, Li-San, and Laursen, E. M., "Shear Measurement Technique for Rough Surfaces," Journal of the Hydraulics Division, American Society of Civil Engineers, vol. 89, No. HY2, March 1963, Part 1, pp. 19-37.

11. Nikuradse, J., "Laws of Flow in Rough Pipes," National Advisory Committee for Aeronautics, TM-1292, 1950, 62 p.